frontiers | Frontiers in Earth Science

TYPE Original Research
PUBLISHED 16 January 2023
DOI 10.3389/feart.2022.1076076

OPEN ACCESS

EDITED BY
Mingjun Zou,
North China University of Water Resources and Electric Power, China

REVIEWED BY
Xin Li,
Xinjiang University, China
Haihai Hou,
Liaoning Technical University, China
Niu Qinghe,
Shijiazhuang Tiedao University, China

*CORRESPONDENCE
Meng Li,
limeng@hpu.edu.cn

SPECIALTY SECTION
This article was submitted to Economic Geology, a section of the journal Frontiers in Earth Science

RECEIVED 21 October 2022
ACCEPTED 04 November 2022
PUBLISHED 16 January 2023

CITATION
Li M, Li M, Pan J, Gao D and Cao Y (2023), Coalbed methane accumulation, in-situ stress, and permeability of coal reservoirs in a complex structural region (Fukang area) of the southern Junggar Basin, China. *Front. Earth Sci.* 10:1076076. doi: 10.3389/feart.2022.1076076

Coalbed methane accumulation, in-situ stress, and permeability of coal reservoirs in a complex structural region (Fukang area) of the southern Junggar Basin, China

Meng Li[1,2]*, Mingjie Li[1,2], Jienan Pan[1,2], Di Gao[1,2] and Yunxing Cao[1,2]

[1]School of Resources and Environment, Henan Polytechnic University, Jiaozuo, China, [2]Collaborative Innovation Center of Coalbed Methane and Shale Gas for Central Plains Economic Region, Henan, Jiaozuo, China

The enrichment of coalbed methane (CBM), *in-situ* stress field, and permeability are three key factors that are decisive to effective CBM exploration. The southern Junggar Basin is the third large CBM basin in China but is also known for the occurrence of complex geological structures. In this study, we take the Fukang area of the southern Junggar Basin as an example, coalbed methane accumulation and permeability, and their geological controls were analyzed based on the determination of geological structures, *in-situ* stress, gas content, permeability, hydrology and coal properties. The results indicate that gas contents of the Fukang coal reservoirs are controlled by structural framework and burial depth, and high-to-ultra-high thickness of coals has a slightly positive effect on gas contents. Perennial water flow (e.g., the Baiyanghe River) favors gas accumulation by forming a hydraulic stagnant zone in deep reservoirs, but can also draw down gas contents by persistent transportation of dissolved gases to ground surfaces. Widely developed burnt rocks and sufficient groundwater recharge make microbial gases an important gas source in addition to thermogenic gases. The *in-situ* stress field of the Fukang area (700–1,500 m) is dominated by a normal stress regime, characterized by vertical stress > maximum horizontal stress > minor horizontal stress. Stress ratios, including lateral stress coefficient, natural stress ratios, and horizontal principal stress ratio are all included in the stress envelopes of China. Permeability in the Fukang area is prominently partitioned into two distinct groups, one group of low permeability (0.001–0.350 mD) and the other group of high permeability (0.988–16.640 mD). The low group of permeability is significantly formulated by depth-dependent stress variations, and the high group of permeability is controlled by the relatively high structural curvatures in the core parts of synclines and the distance to the syncline core. Meanwhile, coal deformation and varying dip angles intensify the heterogeneity and anisotropy of permeability in the Fukang area. These findings will promote the CBM recovery process in China and improve our understanding of the

interaction between geological conditions and reservoir parameters and in complex structural regions.

KEYWORDS

gas content, permeability, *in-situ* stress, burnt rocks, hydrogeology, structural curvature, coal deformation

1 Introduction

Recovery of coalbed methane (CBM) from coal seams can not only benefit mining safety, reduce greenhouse gas emissions, and also increase clean energy supply (Karacan et al., 2011; Moore, 2012). In the Junggar Basin, the CBM resources have been estimated at 3.83 trillion cubic meters, which is the third largest CBM basin in China after the Qinshui Basin and Ordos Basin (Fu et al., 2016; Ou et al., 2018; Yu and Wang, 2020). Exploration of CBM in the Junggar Basin has made significant progress in recent years, among which the Fukang area of the southern Junggar Basin is one of the most successful and typical representatives. The previous investigation demonstrated that coal seam gas-in-place (GIP) resources in the Fukang area are about 682×10^8 m^3, which account for more than twenty percent of the known CBM resources in the southern Junggar Basin (Yang et al., 2005; Ou et al., 2018). The highest daily gas production of vertical wells in China, 27,896 m^3, was archived and gas production has reached 100 million cubic meters annually in this area (Cao et al., 2012; Zhang B et al., 2021). However, before the massive CBM development of this area, coal mining safety issues once seriously threatened coal mining activities in this area because of the coal-and-gas-outburst risks. About 83 workers were killed in the coal-and-gas-outburst accident at the Qimei No.2 mine in 2005 (Yin, 2009), and among the 29 coal mines in the Fukang area, 13 of them are outburst-prone coal mines (Figure 1). Despite the abundant CBM resources, severe coal mining safety situation, and active CBM exploration activities in the Fukang area, complex geological conditions, like, complicated tectonic structures, varying *in-situ* stress, large dip angle, occurrence of deformed coals and widely-developed burnt rocks all make this area a special CBM development case and has aroused great interests among researchers. Understanding how these factors control gas accumulation and permeability, which are critical to CBM exploration and development, is urgent to be solved.

Sedimentology, organic geochemistry, and petroleum and gas potential of Jurassic coal measures in the Junggar Basin, NW China were firstly investigated by Graham et al. (1990), Hendrix et al. (1992) and Chen et al. (1998). Recently, diverse databases have been reported on the geology and reservoir properties of coal reservoirs in the complex structural regions of the southern Junggar Basin. In terms of gas enrichment and origin, Fu et al. (2016), Ou et al. (2018), and Yu and Wang (2020) evaluated the CBM potential of the southern Junggar Basin. Zhi et al. (2013), Fu et al. (2019), Fu et al. (2021) and Wang et al. (2022) investigated the origin and distribution of coalbed gas in the Jurassic coal reservoirs from different parts of the southern Junggar Basin by isotopic and compositional analysis. Several enrichment patterns were further proposed by Li et al. (2018) and Hou et al. (2021). In the aspect of coal properties, Wang et al. (2018) and Zhang T et al. (2021) studied the permeability anisotropy of high-dipping coals from the southern Junggar Basin based on laboratory experiments and numerical simulations. Li et al. (2019) and Fu et al. (2020) reported several datasets of *in-situ* stress from the eastern part of the southern Junggar Basin and discussed vertical permeability trends. Zhou et al. (2016) and Li et al. (2017) conducted experimental studies on the pore structure characteristics of coals in the southern Junggar Basin. Meanwhile, Kang et al. (2020, 2022) studied the in-seam variation of permeability and coal structures through analysis of geophysical Logging in the western Fukang area, southern Junggar Basin.

Although significant contributions have been made by previous researchers, these published studies were mostly experimental research or investigations based on unilateral production data, and important issues concerning gas accumulation and permeability, and their geological controls from tectonic structures, *in-situ* stress, hydrology, burnt rocks, and coal deformation in the complex structural region are thus far poorly understood due to a lack of sufficient data. In this study, we take the Fukang area of the southern Junggar Basin as an example, 55 datasets of field-measured gas contents, 141 datasets of permeability by injection/fall-off well tests, eight datasets of *in-situ* stress by multi-cycle hydraulic fracturing tests, 11 datasets of gas composition were determined, combined with observation and statistics of tectonic structures, fractures/macro-fractures, burnt rocks, coal macerals, and hydrological conditions, we hope to address important issues mentioned above, and further the understanding of gas accumulation and heterogeneity of permeability of the steep-dipping coals in complex structural regions. This work will contribute to the CBM exploration of the southern Junggar Basin, northwestern China, and other CBM basins with complex geological structures.

2 Geological setting

2.1 Tectonic background

The Fukang area is located in the eastern part of the southern Junggar Basin, with an East-West extension of

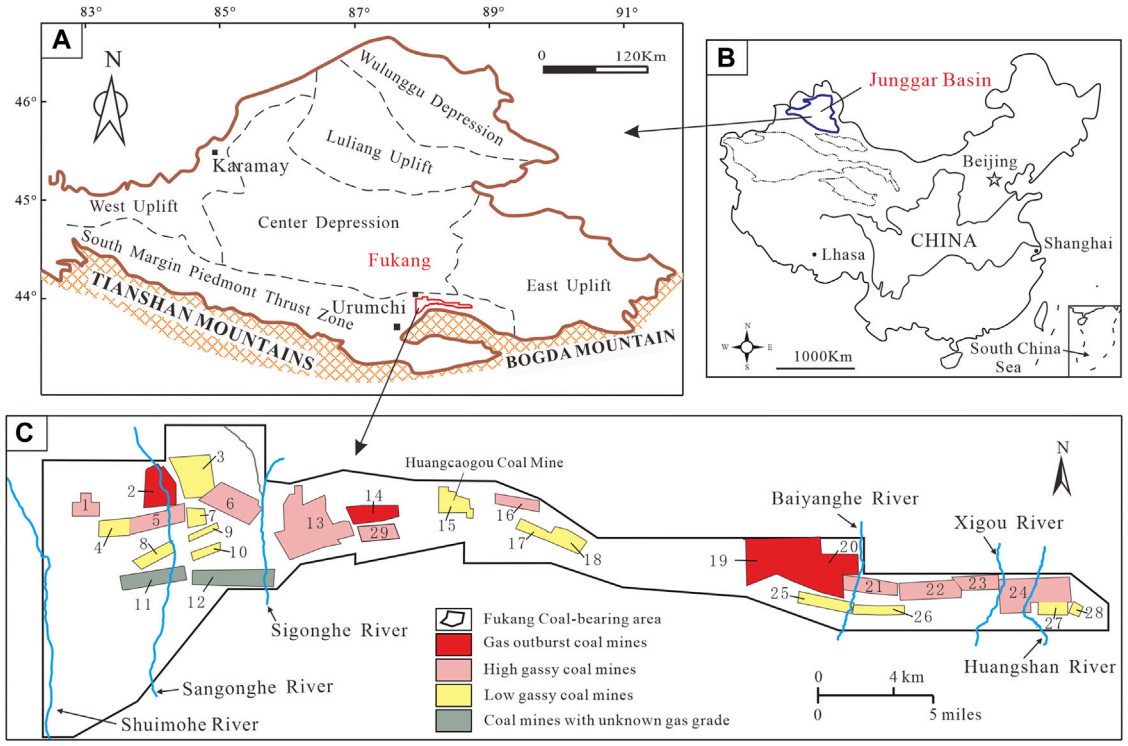

FIGURE 1
(A)-Geographical location of the Junggar Basin. China. **(B)**-Tectonic units of the southern Junggar Basin and location of the Fukang area. **(C)**-Distribution of major coal mines and its potential of coal-and-gas outburst in the Fukang area. (1-Mopangou mine, 2- Qimei No. 2 mine, 3-Dingjiawan mine, 4-Gangou mine, 5-Xinshiji mine, 6-Qimei No. 1 mine, 7-Taipingtan mine, 8-Guangyuan mine, 9-Liuyun mine, 10-Sangongjianjiang mine, 11-Tianchi No. 1 mine, 12-Tianchi No. 3 mine, 13-Wugongmine, 14-Xiaohuangshanmine, 15-Huangcaogou mine, 16-Jinlong mine, 17-Xinlong mine, 18-Kanglong mine, 19-Shizhuanggou mine, 20-Quanshuigoumine, 21-Dahuangshan No. 3 mine, 22-Xigou No. 1 mine, 23-Xigou No. 2 mine, 24-Dahuangshan No. 1 mine, 25-Jintai No. 1 mine, 26-Jintai No. 2 mine, 27-Dongfengfusheng mine, 28-Dahuangshan mine, 29-Choumeigou mine).

57 km and a North-South extension of 3–15 km (Figure 1). The total coal-bearing area is approximately 310 km^2. The Fukang area is tectonically situated in the eastern portion of the south margin piedmont thrust zone of the Junggar Basin (also known as North Bogda Mountain Thrust Zone; Hu et al., 2010; Wu, 1989), and is characterized by a series of compressional synclines and anticlines sandwiched by the two approximately parallel boundary faults, including the Fukang Reverse Fault to the north and the Yaomoshan Reverse Fault to the south. Abundant secondary reverse faults that strike south and southeast are present in these folds and are cut by a series of strike-slip faults (Figure 2; Yang and Tian, 2011; Yin, 2009).

Fault and fold intensity generally increase westward, with the most intense folds and faults occurring at the central portion of the Fukang area, that is, the arcuate structural zone. Compressional thrust from the south by the Bogda Mountain has resulted in large formation dipping angles in the Fukang area, averaging greater than 40°. Coal-bearing strata in the north limbs of these synclines dip towards the south or southeast with an angle of 20°–55°, whereas for strata in the south limbs, the dip is generally 30°–85°NW, or even reverses (Figure 2).

2.2 Coal-bearing sequences and coal seams

Coal-bearing sequences were deposited along the southern Junggar Basin due to tectonic extension and subsidence during the Early and Middle Jurassic, when warm and humid climates were developed (Graham et al., 1990; Carroll et al., 2010; Hou et al., 2022a). The Lower and Middle Jurassic coal-bearing sequences of the southern Junggar Basin have a total thickness of about 2000 m (~6,600 ft). In the Fukang area, coal measures consist of the Lower Jurassic Badaowan Formation and Sangonghe Formation, and the overlying Xishanyao Formation of the Middle Jurassic (Figure 3). The

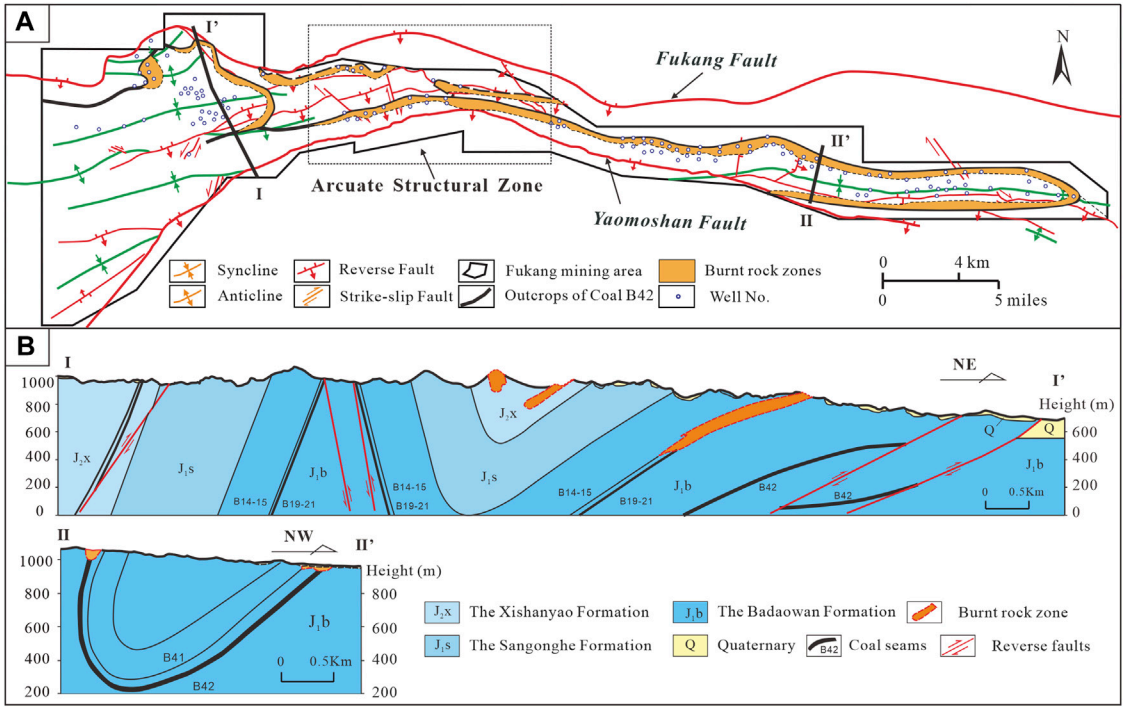

FIGURE 2
Structure outline map **(A)** and two cross-sections **(B)** of the Fukang area showing the occurrences of major faults, folds and coal seams, and distribution of burnt rock zones.

Badaowan Formation is characterized by thick coal seams interbedded with coarse-grained clastic rocks, which were deposited in fluvial deltaic and lacustrine environments (Hendrix et al., 1992; Hou et al., 2020). The younger Sangonghe Formation is typically composed of mudstones, siltstones, medium-to-coarse sandstones, and conglomerates, deposited on the alluvial and flood plains. The Xishanyao Formation consists of sandstones, siltstones, mudstones, and thick coal seams, which are of fluvial-deltaic origin (Hendrix et al., 1992; Hou et al., 2022b).

The Badaowan and Xishanyao formations are the major coal-bearing strata in the study area. Up to 44 coal seams, namely, Nos. B44 to B1, from bottom to top, occur in the Badaowan Formation. The Xishanyao Formation includes 45 coal seams, namely, Nos. X45 to X1 from bottom to top. Due to differential erosion, the Xishanyao Formation is only residual to the west of the Sigonghe River in the study area. Considering the stability and depth of coal as well as coal reservoir properties, gas exploration, and production, by now, were dominantly targeted in the Badaowan Formation in the Fukang area.

Due to the widespread outcropping of coal seams and extremely hot and dry weather of northwestern China, spontaneous combustion of coals occurred frequently in the shallow part of the Fukang area, which led to the formation of coke, and hard, tight, porous burnt rocks which constitute the burnt rock zones in the shallow subsurface area (Figure 4A). Burnt rock zones were frequently developed in the Fukang area and have a strong ability for water storage. In the west part, burnt rock zones are distributed in the limb portion of the Fukang Syncline and the axis portion of the South Fukang Anticline with a width of 30–120 m and a depth of 50–250 m. In the east part, burnt rock zones occur along the north coal outcrops with a width of 30–170 m and with a depth of 250–590 m (Figures 2, 5, 6).

2.3 Characteristics of coal reservoirs

The major coal seams of the Badaowan Formation for coalbed methane exploration are Nos. B14-B15, B19-B21, B39, B41, B42, B43, and B44 coals, of which No. B42 coal is the most stable and continuous seam and has been given priority for fracturing and recovery (Figure 3). But all these major seams are thick (3.5–8.0 m) to ultra-thick (greater than 8 m) coals, with an average accumulated thickness of 76.76m, and are widespread in the entire study area. Nos. B14-15, B19-21, B42, and B44 coal seams are ultra-thick coal and have average thicknesses of 19.48, 8.22, 16.54, and 16.33 m respectively. Nos. B39, B41, and B43 coals are thick coal seams, with an average thickness of 5.60, 5.18, and 5.41 m respectively. The thickness of the No.

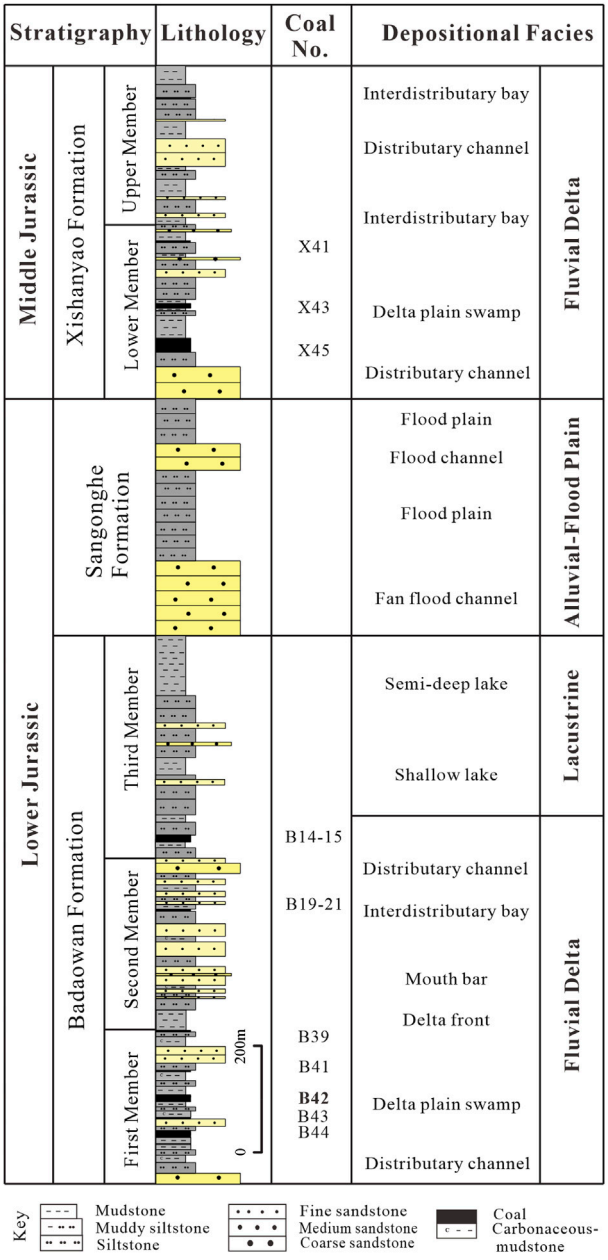

FIGURE 3
Stratigraphic column of the Lower-Middle Jurassic coal-bearing sequences in the Fukang area, southern Junggar Basin, China.

B42 coal ranges between 3.5 and 51.0 m, with an average thickness of 18.5 m. A prominent increasing trend of coal thickness of Coal B42 is recognized (from less than 6.0 to 51.0 m), with coals thicker than 30 m (depocenter) situated in the west part of the study area (Figure 5). Meanwhile, economic coals of the Xishanyao Formation include Nos. X41, X43, and X45 coals with thicknesses averaging 6.74, 18.00, and 33.24 m respectively.

Taking coal No. B42 and X45 as examples, burial depths of coal reservoirs of the Badaowan and Xishanyao Formations were illustrated in Figure 5B and Figure 6B. The burial depth of the Badaowan Formation ranges from zero to about 2000 m (0–6,562 ft) and generally increases towards the south and west, and that of the Xishanyao Formation ranges from zero to about 1000 m. Both burial depths of these two coal measures reach the maximum at the syncline axis portion.

The rank of coals in the Fukang area is dominated by high-volatile C-D bituminous with vitrinite reflectance (Ro) ranging from 0.54% to 0.72%. The macro-lithotype is represented by semi-bright and bright coals. Coal macerals are dominantly composed of vitrinite (ranging from 51.70% to 96.03%) and inertinite (ranging from 0.39% to 45.20%). Exinite is rare and shows a range from 0.1% to 4.94%. The inorganic components of coals consist of carbonate minerals, clay minerals, and pyrites (Supplementary Table S1).

3 Samples and methods

A series of coal cores and blocks were obtained from CBM exploration boreholes as well as underground coal mines in the Fukang area, southern Junggar Basin. Observation of tectonic structures, burnt rocks, fractures, coal deformation, and determination of *in-situ* stress, gas content, and permeability were conducted in the field, while coal composition, vitrinite reflectance, and coalbed gas composition were determined based on collected samples in the laboratory. Vitrinite reflectance measurements were made using a Zeiss microscope with a ×40 oil immersion objective by the national standard of 'Method of determining microscopically the reflectance of vitrinite in coal' (GB/T 6948-2008). Maceral analyses of the samples were made using a point counter by the Chinese National Standard of 'Determination of maceral group composition and minerals in coal' (GB/T 8899-2013). The minimum number of points counted is 500 and the amounts of organic and mineral components determined from point-counting are given as volume percent. Gas contents were determined using the 'direct method', according to the Chinese National Standard of 'Method of determining coalbed gas content' (GB/T 19559-2008). A total of 11 gas samples from field CBM wells in the Fukang area were collected directly from the wellhead. All these gas samples were quantified volumetrically and analyzed for gas composition (CH_4, CO_2, N_2, C_2H_6, and longer-chain hydrocarbons) based on the Chinese National Standard of 'Analysis of natural gas composition-gas chromatography' (GB/T 13610-2014).

The injection/fall-off well test and *in-situ* stress measurements were conducted for the determination of reservoir properties after well completion and before production. The injection/fall-off well test in this study was performed according to the Chinese National Standard of

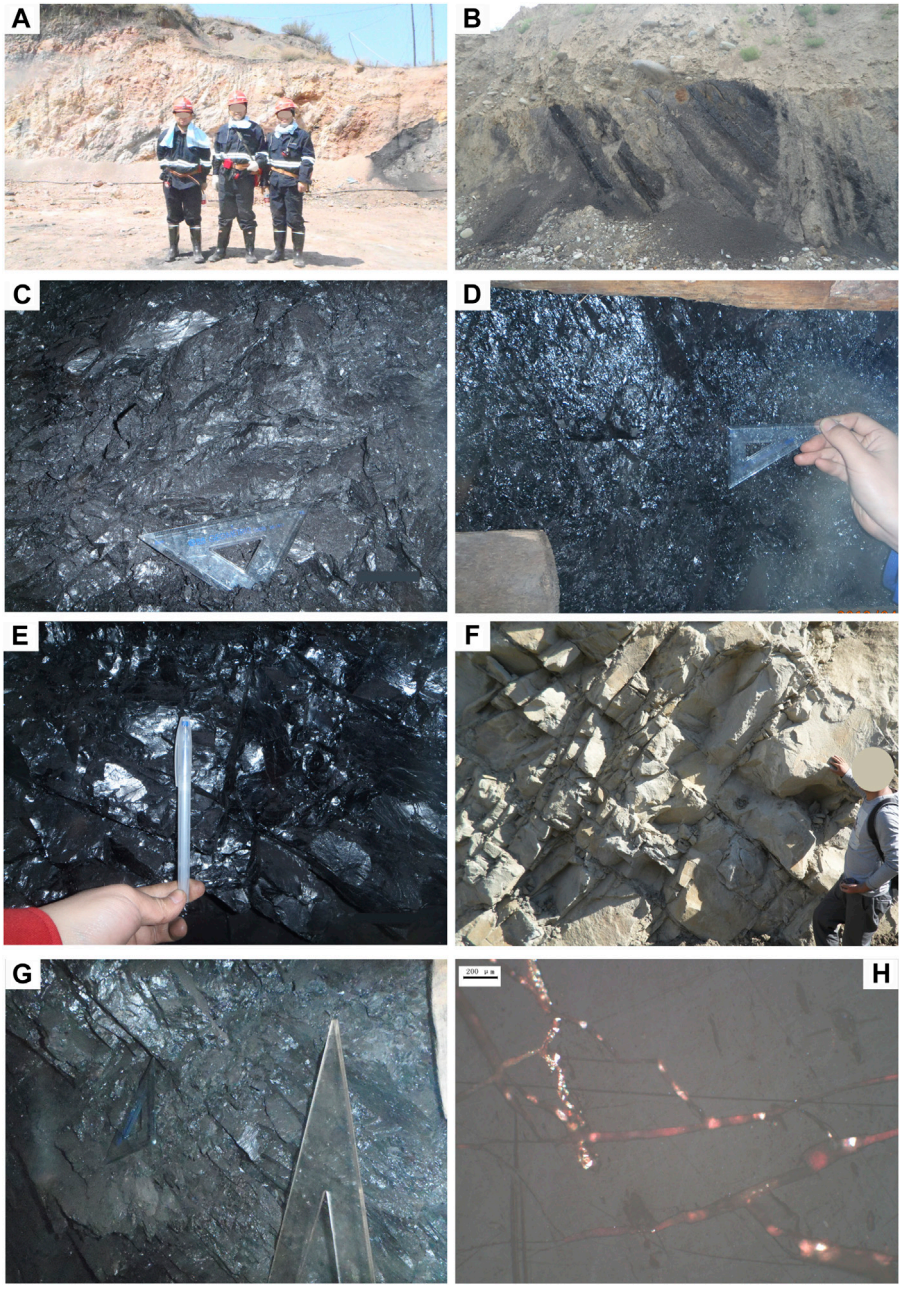

FIGURE 4
Tectonically deformed coals, coal fractures and coal macerals in the Fukang area. **(A)**-Burnt rocks in the Qimei No.1 coal mine. **(B)**-Coal seam outcrops in the western Fukang area. **(C)**-Strong-brittle cataclastic coal in the Huangcaogou mine. **(D)**-Strong-ductile granulated coal in the Wugong mine. **(E,G)**-High-frequency fractures developed in coals from the Jintai No.1 mine **(E)** and Sangongjianjiang mine **(G)**. **(F)**-Well-developed macrofractures at outcrops from Qimei No. 1 mine. **(H)**- Interconnected fractures under microscope of coals from the Qimei No.2 mine.).

'The method of injection/falloff well test for coalbed methane well' (GB/T 24504-2009). Through the injection/fall-off well test process, reservoir parameters including reservoir pressure, permeability, and geothermal status were recorded and calculated. To ensure the accuracy of the data, the well test data in this work were primarily analyzed using the semi-log and log-log curves and were further verified using historical matching pressure curves as discussed by Hopkins et al. (1998). After the injection/fall-off well test, the *in-situ* stress measurements were carried out using multi-cycle hydraulic fracturing tests based on

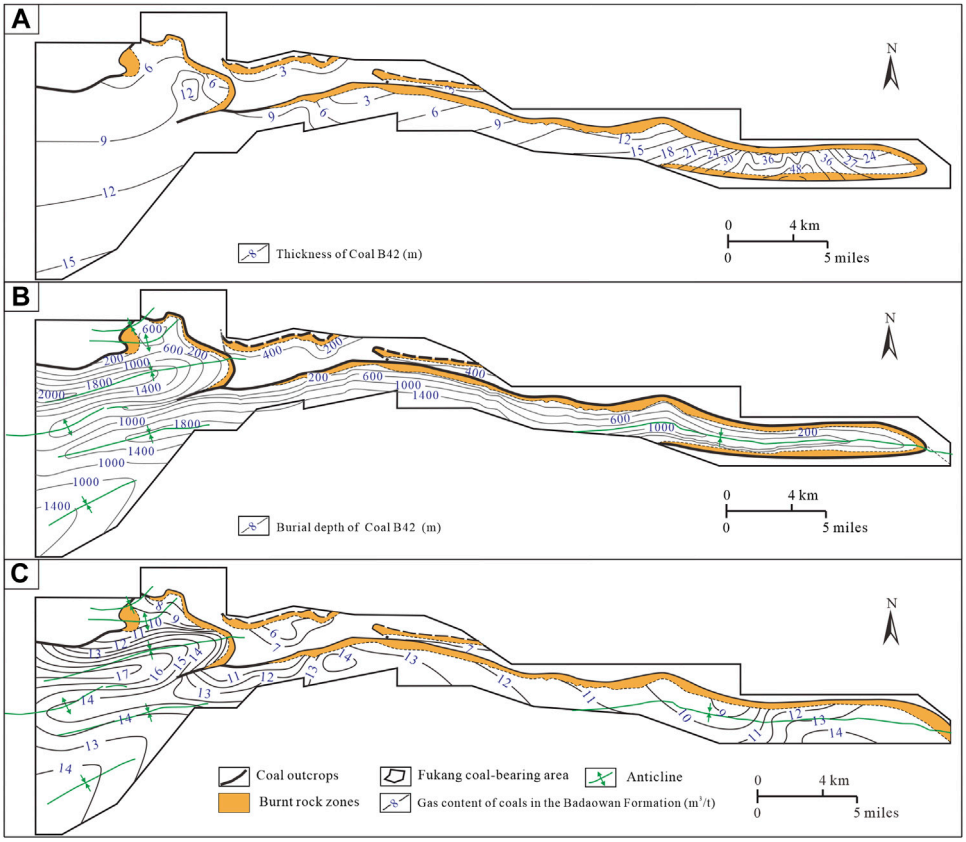

FIGURE 5
Thickness **(A)**, burial depth **(B)** and gas content **(C)** of the Coal B42 of the Badaowan Formation in the Fukang area.

the Chinese Earthquake Industry Standard (DB/T14-2000). To ensure the data are representative and comparable, the measurement of *in-situ* stress was performed for four cycles. During the *in-situ* stress measurement, the balance pressure that can just keep the fracture open is called closing pressure (P_c) and is considered to be equal to the minimum horizontal principal stress (σ_h) (Haimson and Fairhurst, 1970; Haimson and Cornet, 2003),

$$\sigma_h = P_c \tag{1}$$

At the moment a coal seam cracks, because the liquid cannot be timely supplemented, the pressure will greatly decrease; therefore, the critical pressure value recorded by the electric pressure gauge is the breakdown pressure (P_f) of coal seams. According to the theory of elastic mechanics, the maximum horizontal principal stress (σ_H) can be expressed as

$$\sigma_H = 3P_c - P_f - P_o + T \tag{2}$$

where P_f is the breakdown pressure, MPa; P_o is the reservoir pressure, MPa; and T is the tensile strength of coal or rock, MPa.

The vertical stress can be estimated according to the weight of overlying rock as discussed by Hoek and Brown (1980) who combined 116 *in situ* stress test results worldwide and established the prediction formulas of vertical stress (σ_v) as Eq. 3.

$$\sigma_v = 3\gamma D \approx 0.027D \tag{3}$$

where γ is the bulk density of rock in kN/m^3, and D is depth in m.

4 Results

4.1 Gas content

To investigate the gas accumulation of the Fukang coals, the lateral distribution of gas content of the total coal measures in the Badaowan Formation has been illustrated in Figure 5C. Gas contents of coal reservoirs from the Badaowan Formation show a great variation, ranging from about 0.29 to 16.64 m^3/t with an average of 8.15 m^3/t (Supplementary Table S1). Gas contents of the Badaowan Formation are typically greater in the western Fukang area, mostly ranging from 10 to 17 m^3/t, while that of the central and eastern Fukang area is generally from 8 to 14 m^3/t. Variations of gas contents in the Fukang area show clear variation with structure. High gas contents are dominantly

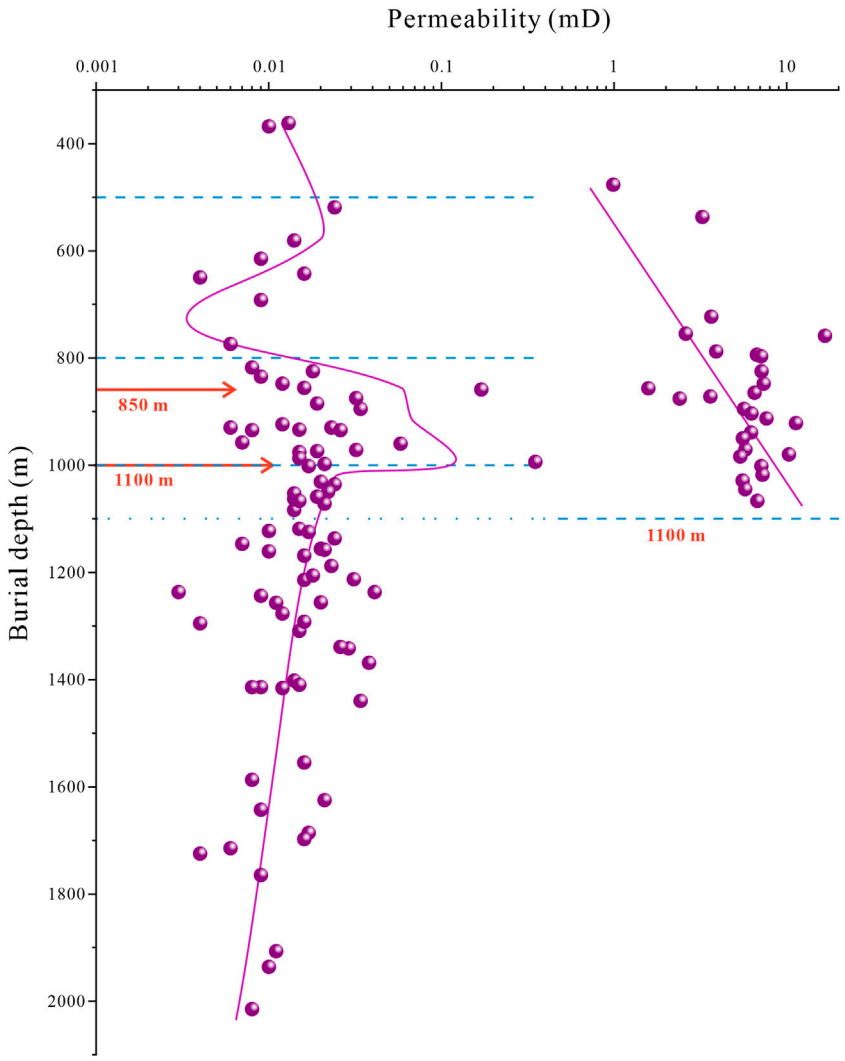

FIGURE 6
Vertical variation of permeability with burial depth.

found in the axis portion of synclines where the burial depths increased dramatically due to the high dip angle of coal seams in the limb portion of the synclines. For example, the highest gas content occurs around the axis portion of the Fukang Syncline, ranging from 14 to 17 m^3/t (Figure 5C). These areas include the Guangyuan mine, Liuyun mine, Sangongjianjiang mine, and Qimei No.1 mine. Meanwhile, the gas content of coal seams adjacent to the outcrop or burnt rock zones generally has gas contents less than 8 m^3/t.

4.2 Permeability

Permeability is a critical control of effective and economical coalbed methane production (Pan et al., 2010; Anggara et al., 2016; Niu et al., 2021). Previous studies illuminated that the permeability of low-to-medium-rank coals is generally favorable despite a high degree of heterogeneity (Wang et al., 2009; Li et al., 2017). The maximum permeability of 16.640 mD was found in the Qimei No.1 mine where the maximum daily gas production of 2.7 × 10^4 m^3/d was achieved in the Fukang area, southern Junggar Basin. On the whole, permeability in the Fukang area shows a high degree of dispersity and is prominently partitioned into two distinct groups behaving different trends with burial depth, one group of high permeability (0.988–16.640 mD) and the other group of low permeability (0.001–0.350 mD) (Figure 6; Supplementary Table S2). In the high permeability group, a positive co-relationship between permeability and depth was found where permeability increases from 1 mD to over 10 mD. However, this group of high permeability only exists

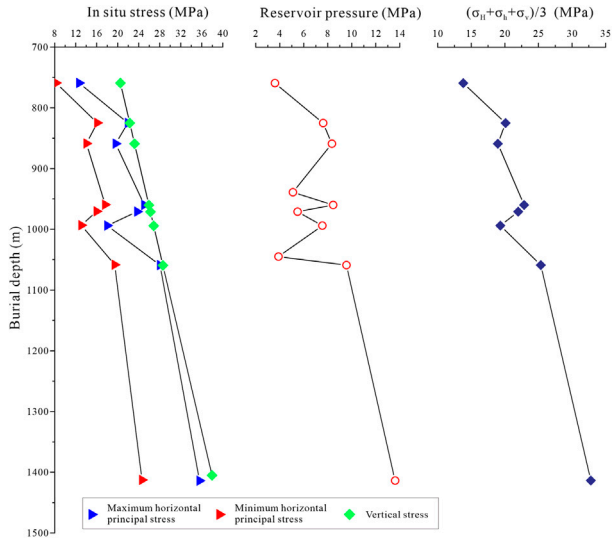

FIGURE 7
Variation of *in-situ* stresses, reservoir pressure and average total stress with depth.

at burial depths shallower than 1,100 m. In the low permeability group, permeability shows different variations as burial depth increases. At depths shallower than 500 m, permeability is generally stable at around 0.01–0.02 mD. From depths of 500–800 m, permeability begins to decrease with depths, and down to an extremely low value (0.004 mD) at depth of around 750 m. From depths of 800–1,000 m, permeability shows an evident increase, and shifts to a relatively high value 'plateau' (≥0.01 mD). Between this high permeability interval, two levels of relatively high permeability occur at depths of 850 and 1,000 m. For coal reservoirs deeper than 1,100 m, permeability shows great dispersion, but a gradually deteriorated trend was found through this strata range, and permeability reduces to extremely low at the deeper reservoirs (0.001 mD ~ 0.01 mD) (Figure 6). In addition, permeability also shows a high degree of variation in the horizontal direction due to different reservoir properties around the Fukang area. Permeability is typically high in the axis portion of the Fukang Syncline and Huangshan Syncline (Figure 7), where permeability is mostly greater than 1 mD even for some deep coal seams (depth > 1000 m).

4.3 *In situ* stress field

With Eqs 1–3, *in-situ* stress of eight datasets were derived from depths between 700 and 1,500 m in the Fukang area, southern Junggar Basin (Supplementary Table S3). The vertical principal stress (σ_v) ranges from 20.49 to 38.18 MPa with an average of 27.04 MPa. The maximum horizontal principal stress (σ_H) is mainly from 12.66 to 35.57 MPa with an average of 23.28 MPa, and its stress gradient is 1.67–2.66 MPa/100 m. The minimum horizontal principal stress (σ_h) is 8.26–24.67 MPa with an average of 16.22 MPa. By an arithmetic average of the maximum horizontal principal stress, minimum horizontal principal stress, and vertical stress, the total average *in-situ* stress (σ_{av}) of the Fukang area was calculated, which is from 13.80 to 32.81 MPa, averaging 22.18 MPa (Figure 8). Compared with the magnitudes of *in situ* stress of the eastern Ordos Basin where σ_{av} is 19.81 MPa, the southern Qinshui Basin where σ_{av} is 18.92 MPa and the western Guizhou where σ_{av} is 15.79 MPa(Meng et al., 2011; Zhao et al., 2016; Chen et al., 2017; Chen et al., 2018), the *in-situ* stress of the Fukang area, southern Junggar Basin is relatively high, which may result from the intense tectonic activities during the Yanshan and Himalaya movements (Li et al., 2019; Fu et al., 2020).

Vertically, the maximum and minimum horizontal principal stresses, and the vertical principal stress are all positively correlated with buried depth with varying trends at specific burial depths. The maximum principal stress and minimum principal stress markedly decrease at depths of 750 m, 850 m, and 1,000 m, while varying trends of vertical stress with depth do not change. The average *in-situ* stress (σ_{av}) also shows evident decreases at depth of 850 and 1,000 m, which means the *in-situ* stress at these levels are relatively low, and this is well coincident with the relatively low values of reservoir pressure between 850 and 1,050 m. It is reasonable to conclude that it is the relatively low *in-situ* stress that contributes to the low

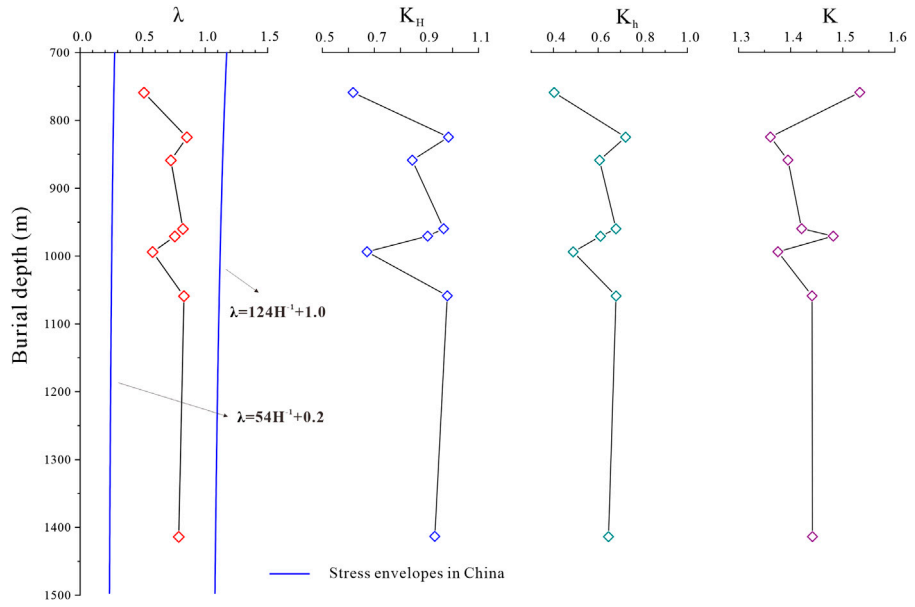

FIGURE 8
Variation of principal stress ratios with depth.

reservoir pressure at these levels. On the whole, the measured results show that the *in-situ* stress of the Fukang area is characterized by $\sigma_v > \sigma_H > \sigma_h$, revealing a normal stress regime (Anderson, 1951; Hoek and Brown, 1980). Although the tectonic structure of the southern Junggar Basin is dominated by a series of thrust fault systems, the current *in-situ* stress regime of the Fukang area, at least from depths of 700–1,500 m, is advantageous for normal faulting activity and indicates an extension zone which is favorable for developing high permeability.

To characterize the variation of *in situ* stress field, several stress ratios, including lateral stress coefficient (λ) and natural stress ratios (K_H and K_h) were introduced (Brown and Hoek, 1978; Hoek and Brown, 1980). The lateral stress coefficient is defined as the ratio of average horizontal principal stress to vertical stress, expressed as

$$\lambda = \frac{\sigma_H + \sigma_h}{2\sigma_v} \quad (4)$$

The natural stress ratios (K_H, K_h) are defined as the effect of tectonic movement on the stress and can be expressed as

$$K_H = \frac{\sigma_H}{\sigma_v} \quad (5)$$

$$K_h = \frac{\sigma_h}{\sigma_v} \quad (6)$$

And the horizontal principal stress ratio (K) reflects the degree of anisotropy of the horizontal stress, expressed as

$$K = \frac{\sigma_H}{\sigma_h} \quad (7)$$

The lateral pressure coefficient (λ) is an effective parameter to characterize the *in-situ* stress distribution characteristics. The lateral pressure coefficient (λ) of coal reservoirs (700–1,500 m) in the Fukang area is in the range of 0.51–0.85, with an average of 0.72, and all the lateral pressure coefficients are included between the *in-situ* stress envelopes of China (Figure 9) (Zhao et al., 2016). Overall, λ is lower than 1, which means that the Fukang CBM reservoirs are dominated by overburden stress. At depths of 750–825 m, λ shows a remarkable increase from 0.51 to 0.85, indicating a vertical-stress-dominated stress regime. From depths >825 m, λ is relatively high (averaging 0.8), except for two levels of low values at 850 and 1000 m, indicating that horizontal stresses begin to play an important role at depths >825 m despite fluctuations of stress field at specific depths. The value of σ_H/σ_v ranges from 0.62 to 0.98 with an average of 0.85, and that of σ_h/σ_v is from 0.40 to 0.72 (average of 0.60). The horizontal principal stress ratio (K) ranges from 1.36 to 1.53, with an average of 1.45, indicating relatively low variation of *in-situ* stress in the horizontal direction (Figure 9).

5 Discussions

5.1 Influencing factors of gas accumulation

5.1.1 Coal thickness and sealing performance

The dissipation of coalbed methane is dominated by diffusion, deriving from differential concentration between

two points (Fick, 1995; Pillalamarry et al., 2011; Fu et al., 2019). Concerning *Fick's Law* and *Principle of Mass Balance*, as coal thickness increases, the time lasting for achieving the median concentration when diffusion is terminated will be lengthened accordingly (Fick, 1995; Pillalamarry et al., 2011). In the Fukang area, a slightly positive correlation between coal thickness and gas contents was revealed which indicates a high resource potential due to the ultra-thickness of the Fukang CBM reservoirs (Figure 10A). Meanwhile, CBM reservoirs are known as 'self-generation and self-accumulation' reservoirs, a well-sealed surrounding condition will undoubtedly improve gas accumulation. The roof of coals in the study area is dominated by mudstones, carbonaceous mudstones, siltstones, and muddy siltstones. Hou et al. (2021) analyzed the surrounding rock condition of coal reservoirs in the middle section of the southern Junggar Basin and subdivided it into four types. The surrounding rocks of the Fukang coals can be classified as Type III and IV which are mainly developed in the distributary bay of the lower deltaic plain and deep-water facies. This indicates a good reservoir sealing performance, and is in favor of the development of high gas content. However, intensely occurring faults increase the likelihood of gas escape through these discontinuous gaps of coal seams. But no evidence shows faults have enhanced gas escaping from coal seams by comparing tectonic structures in Figure 2 and variations of gas contents in Figure 5C, probably due to the compressional properties of the

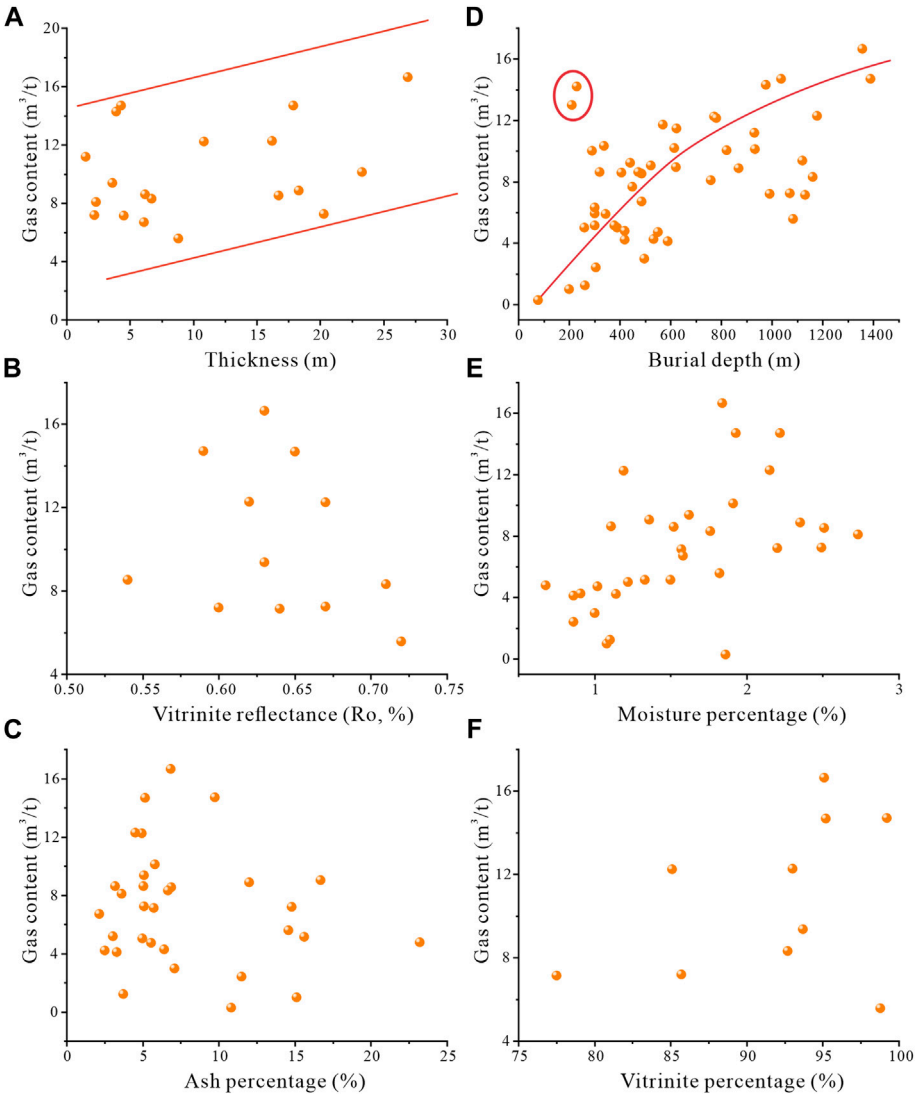

FIGURE 9
Correlations of gas content with coal thickness **(A)**, vitrinite reflectance **(B)**, ash percentage **(C)**, burial depth **(D)**, moisture percentage **(E)**, and vitrinite percentage **(F)**.

occurring reverse faults in the southern Junggar Basin. In addition, steep coal seams in the Fukang area with large dip angles (30°–85°, even reverse) and associated fractures are possible factors that are unfavorable for the preservation of coalbed methane. Decreasing gas contents adjacent to coal outcrops dominatingly resulted from the high dipping properties of coal measures.

5.1.2 Tectonic structure and burial depth

Burial depth has been proven to have a profound effect on gas accumulation which can be summarized into three aspects, 1) reservoir pressure generally increases as deepening burial depth, and gas storage capacity at deep coal reservoirs can be enhanced due to the dominance of adsorption over desorption at high pressures (Faiz et al., 2007; Scott et al., 2007; Xu et al., 2021). 2) gas flow can be limited due to the generally weakened permeability of coal reservoirs in deep positions (as discussed in 4.2), and the increasing distance of gas diffusion and escaping from deep coals to the ground surface is beneficial to gas accumulation (Bustin and Clarkson, 1998; Palmer and John, 1998; Yao et al., 2013; Kang et al., 2020). 3)However, with further increases in depth, temperature increases and will account for more free, soluble gases due to elevated desorption capacity beyond adsorption at high temperatures (Liu et al., 2013; Kang et al., 2018; Fu et al., 2019). As a result, the occurrence of more free, soluble gases adds the chance of gas leakage which might override the positive effects of increased pressures in deep coal reservoirs. As shown in Figure 10B, the gas content of the Fukang coals is positively related to burial depth, but the rate of gas content increase with depth is gradually reduced from depth deeper than 800 m, which might result from the increasing negative effect of elevated temperature. In general, at depths shallower than 600 m gas contents are mainly lower than 8 m^3/t, and at depths greater

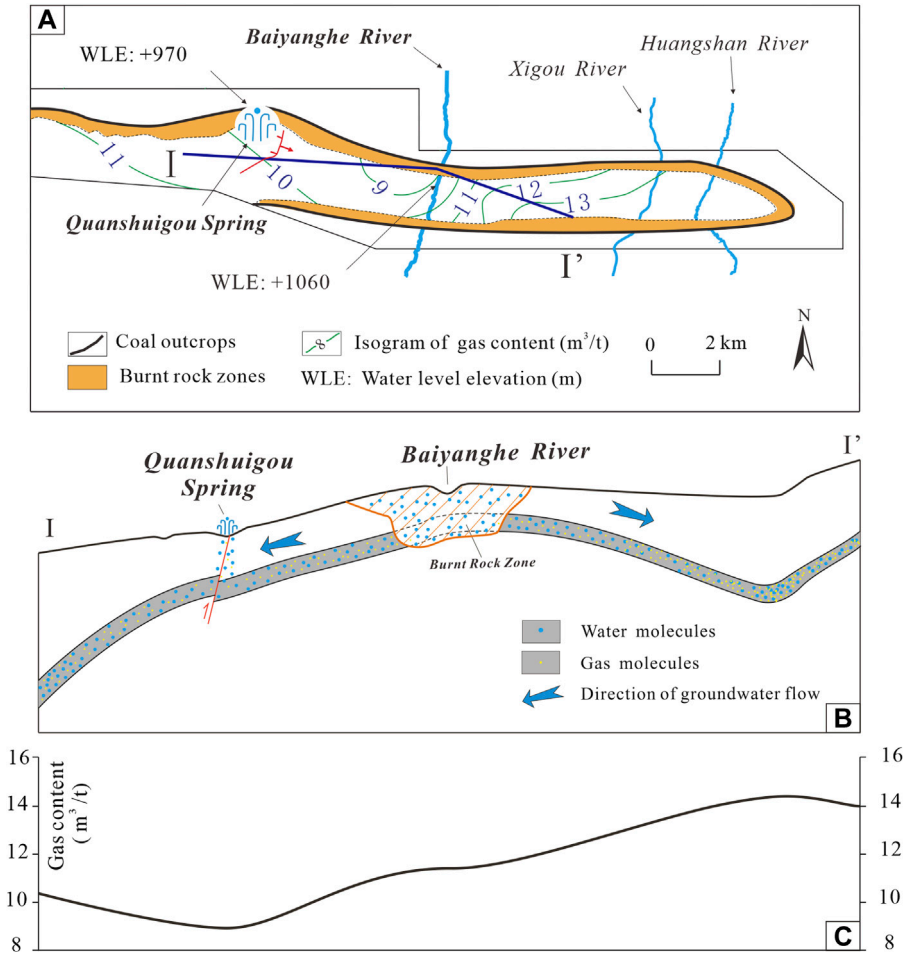

FIGURE 10
Gas accumulation model showing the effect of burnt rock zone, hydrology, biogenic gas formation and coal seam structures on gas contents. **(A)**-Contour map of gas content showing the distribution of geological factors. **(B)**-Diagram of section I-I′ in diagram **(A)** showing migration of coalbed methane and formation water controlled by hydrogeology and tectonic structures. **(C)**-Variation of gas content in section I-I′.

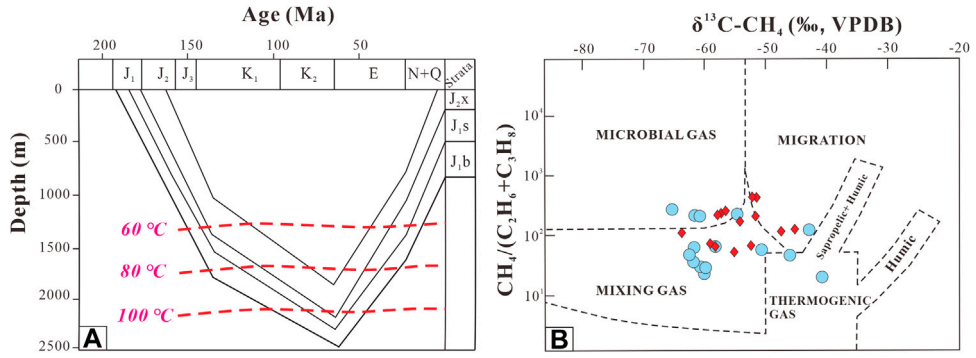

FIGURE 11
(A) Burial history of the southern Junggar Basin, showing basin wide subsidence during the Jurassic-Cretaceous, and Late Cretaceous-Quaternary uplift (modified after Wang et al., 2009). **(B)** Genetic characterization of coalbed methane from the southern Junggar Basin using $\delta^{13}C(CH_4)$ versus hydrocarbon index $[CH_4/(C_2H_6+C_3H_8)]$. Data of blue circles are from Zhi et al. (2013) and that of red diamonds are from Wang et al. (2022). Compositional fields are from Whiticar (1999).

than 600 m gas contents are mostly over 8 m^3/t. However, behind the positive trend between gas content and burial depth, their covariation behaves a large scatter, from which we can infer that combined effects from the three different aspects mentioned above might coexist in the Fukang area. Interestingly, there are two erratic dots at depth of around 250 m in Figure 10B, which exhibit extremely high gas contents (14.21 and 13.00 m^3/t, respectively). Concerning the high gas content at such a shallow burial depth, late-stage biogenic gases might occur in these positions which have been confirmed in literature in the southern Junggar Basin (Hu et al., 2010; Zhi et al., 2013; Wang et al., 2022), and will be discussed in the following section. As a result, late-stage biogenic gases might also contribute to the scatter correlation between gas content and burial depths.

5.1.3 Hydrogeology and burnt rocks

Regional structures and basin hydrodynamics can significantly affect the gas generation and accumulation in coal reservoirs (Bustin and Clarkson, 1998; Pashin, 2010; Gentzis, 2013; Li et al., 2022; Wang et al., 2022). In the Fukang area, groundwater recharges are dominated by glacial melt-water runoff from the Bogda Mountain perennial snow areas, and burnt rock hydrops in the burnt rock zones (Li et al., 2018). Both glacial melt-water runoff and burnt rock hydrops flow down into the deep Jurassic aquifers. Burnt rocks are characteristic of porous fissures which can naturally connect coal outcrops and aquifers in the deep strata (Figures 4A,B). Glacial melt-water runoffs generally flow from south to north and across the coal outcrops, which include the Shuimohe, Sangonghe, Sigonghe, Baiyanghe, and Xigou Rivers in the Fukang area (Figure 1). Worth to note, perennial water flow only exists at the Baiyanghe River which has an average discharge rate of 2.50 m^3/s and a clear flow direction. The Baiyanghe River (water level at +1,060 m) normally occurs as a watershed and forms the groundwater recharge source of the Fukang coal reservoirs (Figure 11). On the west side of the Baiyanghe River, groundwater moves from west to east, through the Baiyanghe River, to burnt rock hydrops, and eventually to the Quanshuigou Springwater outlet (water level at +970 m). In these areas, continuous water flow can transport dissolved coalbed gases away from coal reservoirs to the groundwater, and ultimately to the ground surface. After hundreds of thousands of years of persistent gas loss, gas content can be drawdown to relatively low. For instance, gas content to the west of the Baiyanghe River is generally lower than 10 m^3/t (Figure 11). On the east side of the Baiyanghe River, groundwater flows from east to west, through the Baiyanghe River, to aquifers in the deep part, where a hydraulic stagnant zone was formed. Overpressure in the deep stagnant zone and opposite-direction transportation of water flow compared to gas migration in coal reservoirs can significantly prevent upward gas escaping and favor gas accumulation. As a result, relatively high gas content is developed to the east of the Baiyanghe River, for instance, gas content in the Xigou No.1 and Xigou No.2 mines is generally greater than 11 m^3/t.

5.1.4 External factors

Coal rank and composition are two factors controlling the potential of gas generation (Scott et al., 2007; Yao et al., 2013). However, no clear correlation between gas content and maceral component and coal rank (vitrinite reflectance) was discovered (Figures 10B–F). this may probably result from the narrow range of coal rank, and vitrinite-dominant composition or their effects on gas accumulation were covered by other effects from the factors mentioned above.

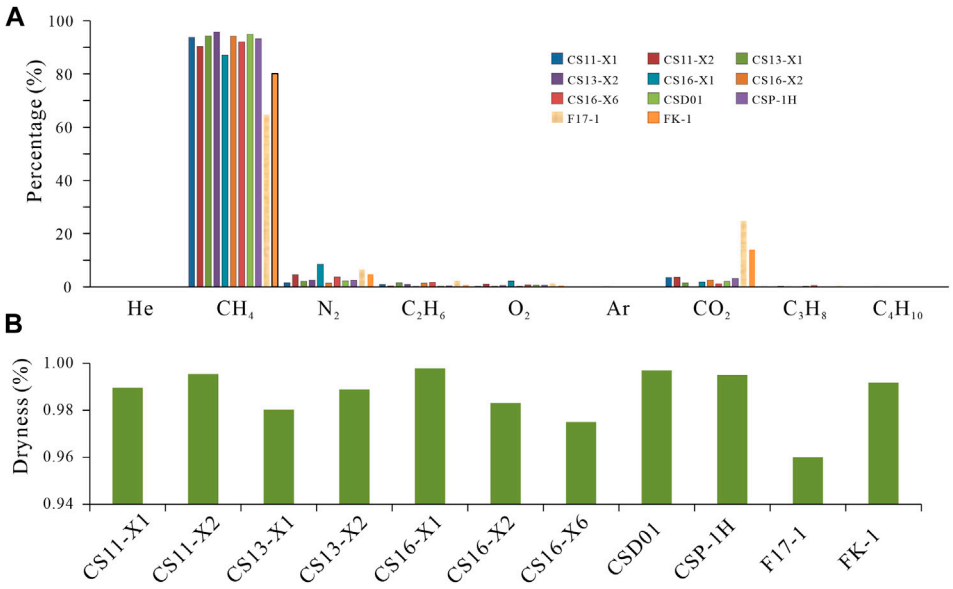

FIGURE 12
Composition **(A)** and dryness **(B)** of coalbed gases in the Fukang area.

5.2 Origins of coalbed methane

The Lower-Middle Jurassic coal-bearing succession in the Fukang area reached its maximum burial depth in the Late Cretaceous when the first coalification event took place, and maximum vitrinite reflectance reached about 0.8% at that age. After the Late Cretaceous, the coal sequences were continuously uplifted and coalification ceased (Chen et al., 1998; Zhi et al., 2013) (Figure 12A). due to differential burial depth, the vitrinite reflectance of the Fukang coals is from 0.54% to 0.72%, which indicates a thermogenic stage of coalbed gas generation. In addition, components of coalbed gases from the desorption of drilling coal cores were determined, which include CH_4, N_2, CO_2, C_2H_6, C_3H_8, C_4H_{10}, Ar, and He (Figure 13). The percentage of methane ranges from 89.16 to 95.78%, and that of carbon dioxide ranges from 0.04% to 24.71%. Air dryness of well extracted gases shows $C_1/C_{1\text{-}5}$ ranges from 0.96 to 1.00, indicating a coal-type, dry gas. These characteristics of coalbed gases further manifest that thermogenic coalbed gases from the Fukang coal reservoirs are mainly thermal degrading gases (Graham et al., 1990; Rice, 1993; Whiticar, 1999).

Recently, carbon isotopic analyses were conducted in the southern Junggar Basin by several researchers. The isotopic composition of methane from the southern Junggar Basin indicated that methane $\delta^{13}C$ value ranges between −41.9‰ and −64.6‰ (Figure 12B) (Hu et al., 2010; Zhi et al., 2013; Wang et al., 2022). In general, thermogenic methane has $\delta^{13}C$ values higher than −55‰ and biogenic methane has values lower than −60‰ because of preferential depleted carbon consumption by methanogens (Whiticar, 1996, 1999; Rice et al., 2008). The Intermediate carbon isotopic value has been interpreted to be a mixture of coexisting biogenic and thermogenic gases (Hu et al., 2010; Fu et al., 2021; Zhang B et al., 2021; Wang et al., 2022). Biogenic gases in the study area have been demonstrated to be dominated by second-stage biogenic gases and a combined microbial pathway of methane generation via both CO_2 reduction and acetate fermentation was proposed by Wang et al. (2022). Fu et al. (2021) pointed out that CO_2 reduction is the main pathway for generating microbial gas based on the identification of bacterial and archaeal16s rRNA genes in formation water (Fu et al., 2021). What is worth noting is that burnt rocks are widely developed around coal outcrops in the Fukang area and other places of the southern Junggar Basin. Freshwater abundant in microorganisms can be easily transported to the deep coal reservoirs through these porous burnt rocks. Coal reservoirs beneath the burnt rock zones, where sufficient groundwater supply exists, can make microbial gases formation for a persistent long period, and high gas content reservoir 'sweet spots' can be developed. High gas content (greater than 13 m^3/t) and methane concentration in the Choumeigou mine confirm the contribution of burnt rocks to gas accumulation in the Fukang area. Wang et al. (2022) further demonstrated that microbial gas is mainly present at depths <800 m, while thermogenic gas primarily occurs at buried depths greater than 1,000 m, and a mixture of the two was present at buried depths of 800–1,000 m. As a result, analyses of widespread burnt rocks and regional hydrodynamic conditions along coal outcrops could be an effective way to

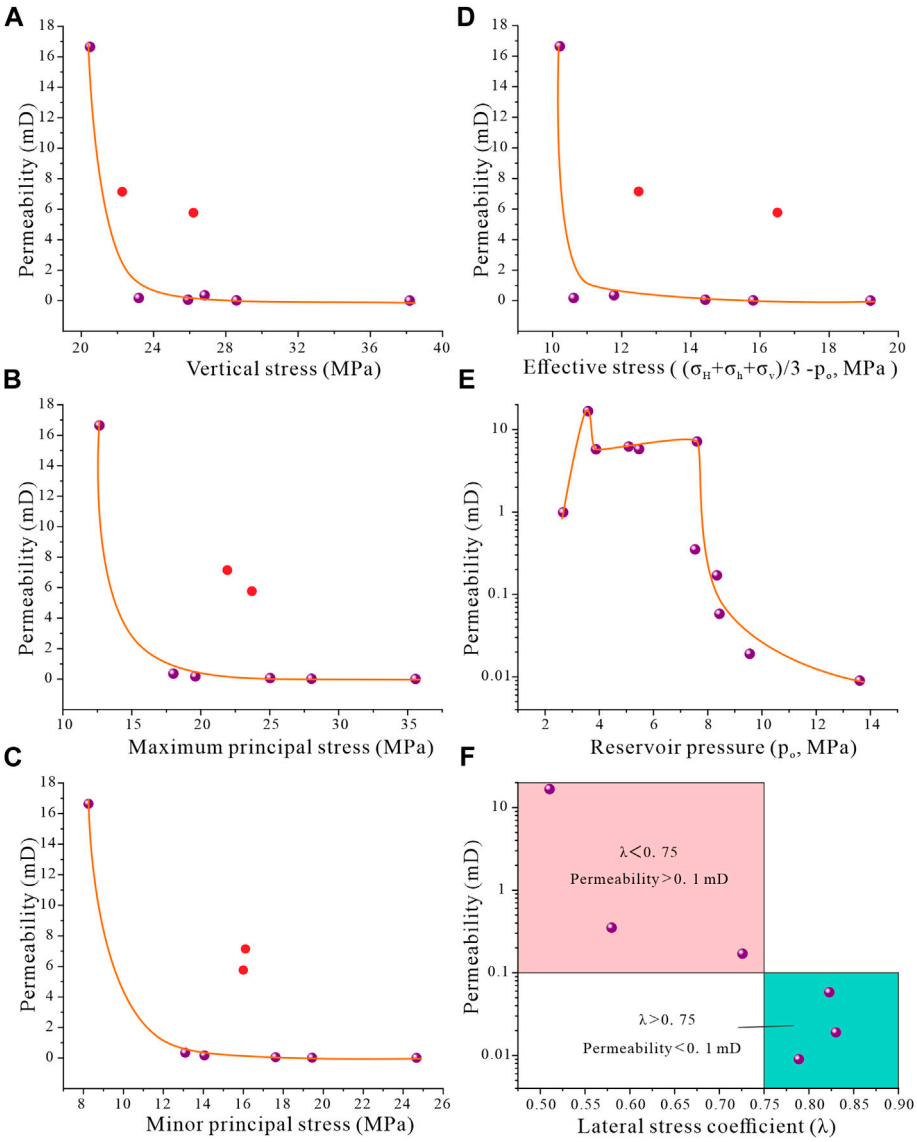

FIGURE 13
Diagram showing influences of in-situ stress field **(A–C)**, effective stress **(D)**, reservoir pressure **(E)**, and lateral stress coefficient **(F)** on permeability.

determine areas with enriched coalbed methane in the southern Junggar Basin.

5.3 Influencing factors of permeability

5.3.1 Fractures/macro-fractures

Naturally occurring fractures in coal are deemed to be the single most important physical attribute governing gas flow in CBM reservoirs (Bustin, 1997; Zhou et al., 2016; Wang et al., 2018; Niu et al., 2022). Fractures are very developed in the Fukang coals, which is consistent with the published cognition that high-density of fractures are generally formed in low-to-medium-rank coals (Dawson and Esterle, 2010; Moore, 2012; Wang et al., 2018). Field observation shows the density of face cleats in the Fukang area ranges from 7 to 49 in every 5 cm while that of butt cleats are from 8 to 29 in every 5 cm (Figure 4H). In addition to these millimeter-centimeter-scale cleats, macro-fractures with magnitude from several centimeters to tens of meters can be obviously found at outcrops in the Fukang area (Figure 4F). Macro-fractures can cut through more than one type of coal sublayers or the whole coal seams. The well-developed

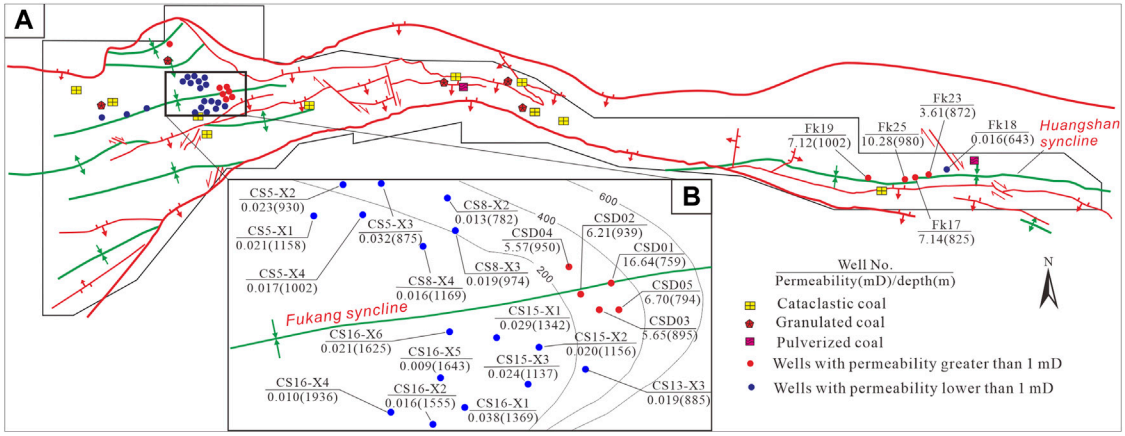

FIGURE 14
(A) Diagram showing distribution of deformed coals and measured permeability of Coal B42 from coalbed methane wells. **(B)** Enlargement of diagram **(A)** at the core part of the Fukang Syncline.

fractures in the Fukang coals of the southern Junggar Basin are partly due to the semi-bright and bright coal (vitrinite group) dominated coal composition on the one hand, and the relatively high intense tectonic stress condition (before present) also has a profound effect on the formation of fractures. Although high-frequency fractures are revealed in the Fukang area, but one thing should bear in mind that all the measurements of fractures are not at the *in-situ* status of geo-stress and depth anymore. The apertures and interconnectedness of the original fractures could be extraordinarily different from the measured fractures. So, *in-situ* permeability determination should be conducted based on analyses of *in-situ* stress, depths, and other external effects. And this appropriately explains why the permeability of the Fukang coals in the southern Junggar Basin exhibit a high range from 0.001 to 16.640 mD despite the high-frequency fractures.

5.3.2 *In-situ* stress

Coal reservoir permeability is basically controlled by fractures and its connectivity, and *in-situ* stress field, but will be dynamically regulated by changing effective stress, matrix shrinkage, and gas slippage during the depletion of CBM wells (Smyth and Buckley, 1993; Pan and Connell, 2011; Chen et al., 2018; Niu et al., 2021; Zhang T et al., 2021). Magnitude, heterogeneity, and anisotropy of initial permeability before CBM production generally determine the potential production rate of CBM wells and have become the core of exploring CBM 'sweet spots' and optimizing CBM well types. Based on measurement of *in-situ* stress and permeability, the influence of *in-situ* stress on the magnitude and heterogeneity of permeability was analyzed. Considering the hydraulic fracturing method adopted in this work cannot be used to derive *in-situ* stress orientation, therefore, the effect of *in-situ* stress on the anisotropy of coal permeability is not included in this paper.

Figures 14A–C shows the relationship between principal stress and permeability. As increases in vertical stress, and maximum and minimum horizontal principal stress, the corresponding permeability perform exponential decline except for two erratic dots (discussed in the following section). Many studies pointed out it was the effective stress that fundamentally formulates the magnitude of permeability (Palmer, 2009; Meng et al., 2011; Liu and Harpalani, 2013). To further quantify the influence of effective *in-situ* stress on permeability, we take the average total *in-situ* stress minus reservoir pressure (P_o) as effective *in-situ* stress (EIS), expressed as,

$$\mathrm{EIS} = \frac{\sigma_v + \sigma_H + \sigma_h}{3} - P_o \tag{8}$$

An exponential decline of permeability with increases in effective stress was discovered in the Fukang area (Figure 14D), which is also verified by the cases from the Qinshui Basin, Ordos Basin, western Guizhou province in China, and other basins of the globe (Jasinge et al., 2011; Meng et al., 2011; Chen et al., 2017; Chen et al., 2018). In the Fukang area, when EIS <11 MPa, permeability dramatically reduces from 16.64 to 0.17 mD with the increase of EIS, which reconfirms the significant effect of effective stress on the permeability of coal reservoirs. When EIS >11MPa, permeability declines to extremely low, mostly below 0.2 mD, which means the major fracture systems in coal seams tend to be closed under high effective stress.

Furthermore, distinct varying trends between lateral stress ratio (λ) and permeability were analyzed here. As shown in

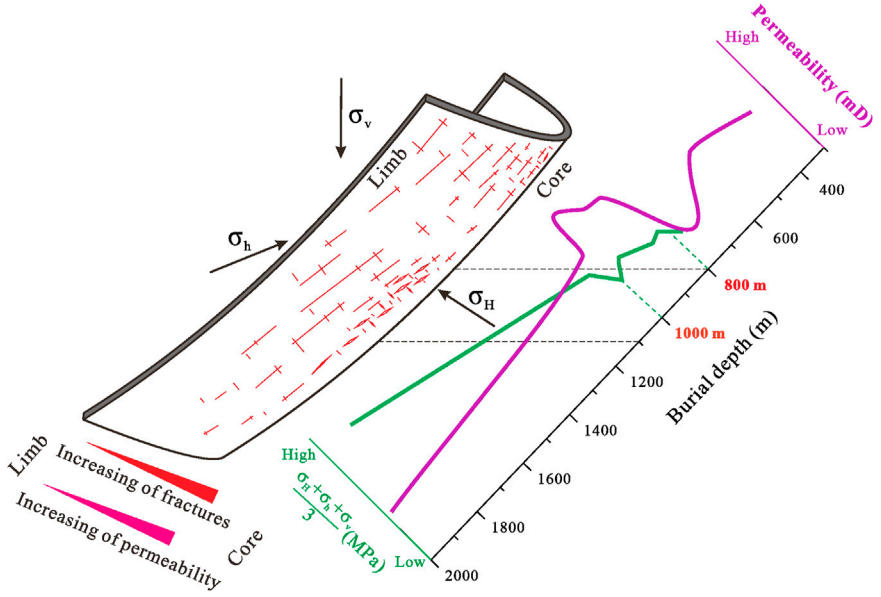

FIGURE 15
Permeability variation model showing the combined effects of *in-situ* stresses and coal structures on permeability in the Fukang area, southern Junggar Basin.

Figure 14F, where $\lambda < 0.75$, permeability is generally greater than 0.1 mD, but when $\lambda > 0.75$, permeability is lower than 0.1 mD. The lateral stress ratio actually reflects the change of the *in-situ* stress regime, when $\lambda < 0.75$, the horizontal stresses are relatively low as vertical stress dominates the *in-situ* stress field, and low stress in the horizontal direction favors the development of relatively high permeability. When $\lambda > 0.75$, the *in-situ* stress from both the horizontal and vertical directions are tending to converge, and the consistency of *in-situ* stress from three directions in a normal faulting stress regime enhanced the compression and closures of fractures in coal reservoirs, which resulted in the relatively low permeability. In addition, the relationship between coal permeability and reservoir pressure was plotted in Figure 14E. When reservoir pressure is low (2–8 MPa), permeability is relatively high (≥1 mD), however, when reservoir pressure is >8 MPa, permeability decreases rapidly to less than 0.2 mD. As shown in Figure 8, low reservoir pressures (2–8 MPa) generally distribute at depths shallower than 1,100 m where the total *in-situ* stress is low. As a result, it can be inferred that it is the low *in-situ* stress (EIS), not the low reservoir pressure, that eventually accounts for the relatively high permeability in the shallower coal seams (<1,100 m).

At the same time, as mentioned above, permeability can be partitioned into two separate groups with distinct relationships with depths, and the low group of permeability performs a distinct variation trend with depth. Associated with vertical variation of *in-situ* stress field, the co-relationship between depth-dependent *in-situ* stress field and permeability was discussed here. At shallower coal reservoirs (depths <500 m), *in-situ* stress measurements in major Chinese coal basins have revealed that *in-situ* stress field at this depth range is dominated by tectonic compression, and the major principal stress normally exhibits the trend of $\sigma_H > \sigma_h > \sigma_v$ (Chen et al., 2017; Chen et al., 2018; Li et al., 2019). As a result, the reverse faulting stress regime reflected by the principal stress field is decisive to the low permeability at depths shallower than 500 m (0.01–0.02 mD) (Figures 6, 8). When coal reservoirs go deeper, *in-situ* stress in the Fukang area shifts to the regime of $\sigma_v > \sigma_H > \sigma_h$, and is dominated by gravitational loading but with distinctive variation of stress field as shown in Figure 8. At depths of 500–800 m, with deepening coal reservoirs, *in-situ* stress increase gradually, and a decreasing trend of permeability with depth were found at this depth range. Then, as burial depth increases, horizontal stress behaves a prominent decline at depths of 800–1,000 m, especially at levels of 850 and 1,000 m, this causes the effective stress acted on coal seams to attenuate, as a result, a relatively high permeability 'plateau' was developed. Finally, as depth increases to deeper than 1,000 m, the *in-situ* stress regime transfers to the normal increasing stress field and persists to decrease with depth, so a persistent decline of permeability was discovered at depths below 1,000 m. Therefore, the variation of permeability of the low permeability group with depths actually reflects the co-

variation between depth-dependent stress field change and permeability.

5.3.3 Geometry and attitude of coal seams

As a layered energy reservoir, the geometry and attitude of coal seams also have a great impact on permeability. The frequency of fractures, apertures, interconnectedness, and orientation of fractures can be quite different in different parts of the coal seams, and all these factors can significantly influence the heterogeneity and anisotropy of reservoir properties. The Fukang area of the southern Junggar Basin is characterized by intense tectonic structures as shown in Figure 2, and varying strike and dip angles shaped the complex attitude and frequently changing morphology of coal seams. Kang et al. (2022) calculated the structural curvature of coal seams in the western Fukang block, which ranges from 0.0001 to 0.005 and can be classified as high structural curvature as discussed by Shen et al. (2010). It is worth noting that in the core parts of folds, where high structural curvature occurs, extraordinary high-frequency fractures and favorable apertures have been developed due to the relatively tensile stress regime (Figures 4E,G; Figure 15). The distribution of measured permeability from CBM wells shows a remarkable increase of permeability in CBM wells in the core parts of synclines compared to that in the lime parts of synclines (Figure 7). Measured permeability from CBM wells in the core parts of synclines is mainly greater than 1 mD, while that in the lime parts of synclines is mostly lower than 0.1 mD. Moreover, the closer to the core of synclines, the higher permeability is prone to be developed. The highest permeability (16.64 mD) has been discovered in the CBM well CSD-01 which is located just at the core of the Fukang syncline. So, it is not difficult to infer that the high group of permeability in Figure 6 represents measured permeability from CBM wells proximal to the fold core, and the correlation between permeability and depths reflects the covariation between measured permeability and the distance from the operating well to the core of the corresponding folds. Additionally, these high permeability dots erratically exhibited in Figures 14A–D are from CBM well CSD03 and Fk17 with permeability of 5.76 mD and 7.14 mD respectively. It can be seen in Figure 14 that both of these two wells are distributed at the core part of the major synclines in the Fukang area, actually, it is the high structural curvature of coal seams that accounts for the high permeability in these coal reservoirs.

Furthermore, the dip angle of the Fukang coal has a high range from 20° to 90°, or even reverse. The orientation of fractures/cleats in coal seams, and the stress and strain of coal reservoirs vary with dip angle changes, and this can significantly increase the anisotropy of permeability. Zhang B et al. (2021) demonstrated that the rate of permeability decrease had a tendency of first decrease and then increase with dip angle gradually increased from 0° to 90°. This will increase the difficulty of permeability prediction and upgrade the uncertainty of optimization of sweet pot for CBM exploration. However, detailed field observations and measurements of fractures and microfracture at outcrops and underground coal mines will help determine the heterogeneity and anisotropy of permeability. Statistical analysis of macro-fractures in the western Fukang area shows that a group of macro-fractures along the strike are more developed than another group of macro-fractures perpendicular to the strata strike, which indicates prevailing permeability will be developed along the strike, and fracturing in the Fukang area should be conducted along this direction.

5.3.4 Coal deformation

Tectonic deformation can lead to obvious alteration of pore-fracture systems in coal reservoirs, and can significantly change the seepage capacity of gas flow (Karacan and Okandan, 2000; Li et al., 2003; Li et al., 2021). Deformation of coal structure in a brittle or cataclastic manner can enhance permeability by the magnitude of 3–8 times above the surrounding reservoir (Li and Ogawa, 2001; Jiang et al., 2010). This kind of relatively weak deformation tends to open up existing cleat apertures and increase their interconnectedness, thus increasing permeability (Kang et al., 2022; Li et al., 2003; Pan et al., 2015). On the contrary, in sheared coals behave in a more ductile or mylonitic manner, permeability has been demonstrated to be dramatically deteriorated (Li and Ogawa, 2001; Li et al., 2021). With mylonitic deformation, the coals tend to be tightly compressed and cleat apertures collapse (Li et al., 2003). These types of shear zones have also been related to a high risk of coal and gas outbursts during mining activities (Li et al., 2016; Pan et al., 2019).

In the Fukang area, tectonic deformation is widely recognized at both outcrops and heading stopes in underground mines. Tectonically deformed coals in this area can be subdivided into cataclastic coals (Deformation in a cataclastic manner), as well as granulated and pulverized coals (Deformation in ductile and mylonitic manners). All three types of deformed coals are dominantly distributed in the central part of the Fukang area, as known as the arcuate structural zone, that is to the west of the Kanglong coal mine and to the east of the Wugong coal mine (Figures 4C,D, 7). In these places, intense tectonic movement and high shearing stress resulted in the high occurrences and intensity of coal deformation. Kang et al. (2022) evaluated in-seam variation of coal structures in the western Fukang area by logging data analyses and found that the whole thick coal seams in the western Fukang area are vertically composed of 5–10 sublayers with different coal structures, and tectonically deformed coals are mainly developed in the lower-middle part of coal seams (Kang et al., 2022). Although the occurrence of cataclastic coals can improve the aperture of fractures/cleats and enhance gas flow in coal seams, unevenly distributed granulated and pulverized coals can profoundly decrease the interconnectedness of fractures/cleats and hinder gas flow. For instance, at the Qimei No.2 mine where granulated coals were developed, extremely low permeability (0.023 mD) was

discovered at CBM well CX5-X2, and a serious coal-and-gas-outburst occurred in 2005. Overall, the development of deformed coals has a profound effect on the permeability heterogeneity of coal reservoirs, which increases the difficulty of coalbed methane stimulation and recovery and increase the ever-existing risk of coal-and-gas-outburst during the underground mining in the Fukang area. CBM exploration and exploitation in the Fukang area should avoid these places where deformed coals were reported.

6 Conclusion

1) Structural framework and burial depth generally control gas contents of coal reservoirs in the Fukang area. Gas contents increase with deepening burial depth, but the rate of gas content increase with depth is gradually reduced due to enhanced negative effects from increased temperature beyond the positive effects from increased pressures in deep coal reservoirs. The high-to-ultra-high thickness of coal reservoirs has a slightly positive effect on gas content.
2) Perennial water flow of the Baiyanghe River is in favor of gas accumulation to the east part of the Baiyanghe River by forming a hydraulic stagnant zone in the deep coal reservoirs. But gas contents can be drawdown by persistent transportation of dissolved coalbed gases to ground surfaces (Quanshuigou Springwater outlet) to the west of the Baiyanghe River. Meanwhile, widely developed burnt rocks make groundwater easily access the deep coal reservoirs, and abundant microorganisms transported to the deep coal reservoirs facilitate the generation of late-stage microbial gases, which, together with thermal degrading gases, account for the origin of coalbed gases in the Fukang area.
3) The *in-situ* stress field of the Fukang area is characterized by vertical stress (σ_v) > maximum horizontal stress (σ_H) > minor horizontal stress (σ_h), indicating a normal stress regime. The maximum principal stress, minimum principal stress, and vertical stress generally increase with depth, but the maximum and minimum principal stress show an evident decline at depths of 850 and 1,000 m. All the stress ratios, including lateral stress coefficient (λ), natural stress ratios (K_H and K_h), and horizontal principal stress ratio (K) are included in the *in-situ* stress envelopes of China.
4) Permeability in the Fukang area shows a high degree of dispersity, ranging from 0.001 to 16.640 mD, and is prominently partitioned into two distinct groups, one group of high permeability (0.988–16.640 mD) and the other group of low permeability (0.001–0.350 mD). The low group of permeability is prominently formulated by depth-dependent stress field change. At depths of 500–800 m, permeability gradually decreases with increasing *in-situ* stress as burial depth deepens. From 800 to 1000 m, horizontal principal stresses behaved a prominent decline which contribute to a relatively high permeability 'plateau'. At depths deeper than 1,000 m, a persistent decline of permeability occurs with deepening burial depth. For the high group of permeability, relatively high structural curvature in the core parts of synclines, and the distance to the syncline core significantly dominate permeability in the Fukang area.
5) Furthermore, permeability shows exponential decline with increasing effective *in-situ* stress and lateral stress ratio (λ) has a profound effect on permeability. When $\lambda < 0.75$, permeability is generally greater than 0.1 mD while permeability is lower than 0.1 mD when $\lambda > 0.75$. Frequently occurring deformed coals increase the difficulty of coalbed methane stimulation and recovery. High-ranging dip angle of the Fukang coal seams can dramatically increase the anisotropy of permeability. Analysis of the attitude of fractures/macro-fractures will favor the determination of preferred fracturing orientation and optimizing CBM well types.

Data availability statement

All data discussed in the paper will be made available in the Supplementary Material, further inquiries can be directed to the corresponding author.

Author contributions

ML and MiL are responsible for writing original manuscript. JP and YC are responsible for copyright and revising the manuscript. DG is responsible for drawing figures and data arrangement. DG and MiL is responsible for basic data and maps. ML, DG, and MiL are responsible for field and lab work.

Funding

This research was funded by the National Natural Science Foundation of China (No. 41502108, 41772162), China Postdoctoral Science Foundation (No. 2016T90667) and the Key Research Project of Universities of Henan Province (No. 20A170008).

Acknowledgments

We are grateful to Xuesong Yang from the Xinjiang Cleanseed New Energy Company for the help of field work and data collection and Yawen Wu and He Zhou from Henan Polytechnic University for the analysis of gas contents. Professor Jiangfeng Chen from Henan Polytechnic University is thanked for supplying the hydrogeological data.

Conflict of interest

The authors declare that the research was conducted in the absence of any commercial or financial relationships that could be construed as a potential conflict of interest.

Publisher's note

All claims expressed in this article are solely those of the authors and do not necessarily represent those of their affiliated organizations, or those of the publisher, the editors and the reviewers. Any product that may be evaluated in this article, or claim that may be made by its manufacturer, is not guaranteed or endorsed by the publisher.

Supplementary material

The Supplementary Material for this article can be found online at: https://www.frontiersin.org/articles/10.3389/feart.2022.1076076/full#supplementary-material

References

Anderson, E. M. (1951). *The dynamics of faulting and dyke formation with applications to britain*. Second edition ed. Oliver and Boyd, Edinburgh.

Anggara, F., Sasaki, K., and Sugai, Y. (2016). The correlation between coal swelling and permeability during CO2 sequestration: A case study using kushiro low rank coals. *Int. J. Coal Geol.* 166, 62–70. doi:10.1016/j.coal.2016.08.020

Brown, E. T., and Hoek, E. (1978). Trends in relationships between measured *in-situ* stresses and depth. *Int. J. Rock Mech. Min. Sci. Geomechanics Abstr.* 15, 211–215. doi:10.1016/0148-9062(78)91227-5

Bustin, R. M., and Clarkson, C. R. (1998). Geological controls on coalbed methane reservoir capacity and gas content. *Int. J. Coal Geol.* 38, 3–26. doi:10.1016/s0166-5162(98)00030-5

Bustin, R. M. (1997). Importance of fabric and composition on the stress sensitivity of permeability in some coals, northern sydney basin, Australia: Relevance to coalbed methane exploitation. *AAPG Bull.* 81, 1894–1908.

Cao, Y., Yang, X., He, M., Tian, l., and Shi, b. (2012). *Evaluation and development technology of pilot Project selection for coalbed methane in low-rank coals of the Fukang mining area, Xinjiang uygur autonomous region*. Xinjiang Cleanseed New Energy Co., Ltd and Henan Polytechnic University, Jiaozuo, China 118.

Carroll, A. R., Graham, S. A., and Smith, M. E. (2010). Walled sedimentary basins of China. *Basin Res.* 22, 17–32. doi:10.1111/j.1365-2117.2009.00458.x

Chen, J., Zhao, C., Wang, Z., He, z., and Qin, Y. (1998). Organic geochemical characteristics of oil, gas and source rocks of Jurassic coal measures in Northwestern China. *Geol. Rev.* 44, 149–158.doi:10.1016/j.jnggs.2019.11.003

Chen, S., Tang, D., Tao, S., Xu, H., Li, S., Zhao, J., et al. (2017). *In-situ* stress measurements and stress distribution characteristics of coal reservoirs in major coalfields in China: Implication for coalbed methane (CBM) development. *Int. J. Coal Geol.* 182, 66–84. doi:10.1016/j.coal.2017.09.009

Chen, S., Tang, D., Tao, S., Xu, H., Zhao, J., Fu, H., et al. (2018). *In-situ* stress, stress-dependent permeability, pore pressure and gas-bearing system in multiple coal seams in the Panguan area, Western Guizhou, China. *J. Nat. Gas Sci. Eng.* 49, 110–122. doi:10.1016/j.jngse.2017.10.009

Dawson, G. K. W., and Esterle, J. S. (2010). Controls on coal cleat spacing. *Int. J. Coal Geol.* 82, 213–218. doi:10.1016/j.coal.2009.10.004

Faiz, M., Saghafi, A., Sherwood, N., and Wang, I. (2007). The influence of petrological properties and burial history on coal seam methane reservoir characterisation, Sydney Basin, Australia. *Int. J. Coal Geol.* 70, 193–208. doi:10.1016/j.coal.2006.02.012

Fick, A. (1995). On liquid diffusion. *J. Memb. Sci.* 100, 33–38. doi:10.1016/0376-7388(94)00230-v

Fu, H., Tang, D., Pan, Z., Yan, D., Yang, S., Zhuang, X., et al. (2019). A study of hydrogeology and its effect on coalbed methane enrichment in the southern Junggar Basin, China. *Am. Assoc. Pet. Geol. Bull.* 103, 189–213. doi:10.1306/06071817190

Fu, H., Tang, D., Xu, H., Xu, T., Chen, B., Hu, P., et al. (2016). Geological characteristics and CBM exploration potential evaluation: A case study in the middle of the southern Junggar Basin, NW China. *J. Nat. Gas Sci. Eng.* 30, 557–570. doi:10.1016/j.jngse.2016.02.024

Fu, H., Yan, D., Yang, S., Wang, X., Wang, G., Zhuang, X., et al. (2021). A study of the gas-water characteristics and their implications for the coalbed methane accumulation modes in the Southern Junggar Basin, China. *Am. Assoc. Pet. Geol. Bull.* 105, 189–221. doi:10.1306/02282018273

Fu, H., Yan, D., Yang, S., Wang, X., Zhang, Z., and Sun, M. (2020). Characteristics of *in situ* stress and its influence on coalbed methane development: A case study in the eastern part of the southern Junggar Basin, NW China. *Energy Sci. Eng.* 8, 515–529. doi:10.1002/ese3.533

Gentzis, T. (2013). Coalbed methane potential of the Paleocene Fort Union coals in south-central Wyoming, USA. *Int. J. Coal Geol.* 108, 27–34. doi:10.1016/j.coal.2012.06.003

Graham, S. A., Brassell, S., Carroll, A. R., Xiao, X., Demaison, G., Mcknight, C. L., et al. (1990). Characteristics of selected petroleum source rocks, xianjiang uygur autonomous region, northwest China. *AAPG Bull.* 74, 493–512.

Haimson, B. C., and Cornet, F. H. (2003). ISRM suggested methods for rock stress estimation—Part 3: Hydraulic fracturing (HF) and/or hydraulic testing of pre-existing fractures (HTPF). *Int. J. Rock Mech. Min. Sci. (1997).* 40, 1011–1020. doi:10.1016/j.ijrmms.2003.08.002

Haimson, B., and Fairhurst, C. (1970). "*In-situ* stress determination at great depth by means of hydraulic fracturing," in *Rock mechanics - theory and practice*. Editor W. H. Somerton (Amer. Inst. Mining Eng.), New York, NY, USA 559–584.

Hendrix, M. S., Graham, S. A., Carroll, A. R., Sobel, E. R., Mcknight, C. L., Schulein, B. J., et al. (1992). Sedimentary record and climatic implications of recurrent deformation in the Tian Shan: Evidence from Mesozoic strata of the north Tarim, south Junggar, and Turpan basins, northwest China. *Geol. Soc. Am. Bull.* 104, 53–79. doi:10.1130/0016-7606(1992)104<0053:sracio>2.3.co;2

Hoek, E., and Brown, E. T. (1980). *Underground excavations in rock*. CRC Press London, UK.doi:10.1201/9781482288926

Hopkins, C. W., Frantz, J. H., Flumerfelt, R. W., and Spivey, J. P. (1998). Pitfalls of injection/falloff testing in coalbed methane reservoirs. SPE permian basin oil and gas recovery conference. Midland, TX, USA (Society of Petroleum Engineers). 9–24.

Hou, H. H., Shao, L. Y., Tang, Y., Li, Y. N., Liang, G. D., Xin, Y. L., et al. (2020). Coal seam correlation in terrestrial basins by sequence stratigraphy and its implications for palaeoclimate and palaeoenvironment evolution. *J. Earth Sci-China*, 1–24. doi:10.1007/s12583-020-1069-4

Hou, H., Liang, G., Shao, L., Tang, Y., and Mu, G. (2021). Coalbed methane enrichment model of low-rank coals in multi-coals superimposed regions: A case study in the middle section of southern Junggar Basin. *Front. Earth Sci.* 15, 256–271. doi:10.1007/s11707-021-0917-6

Hou, H., Shao, L., Li, Y., Liu, L., Liang, G., Zhang, W., et al. (2022a). Effect of paleoclimate and paleoenvironment on organic matter accumulation in lacustrine shale: Constraints from lithofacies and element geochemistry in the northern Qaidam Basin, NW China. *J. Petroleum Sci. Eng.* 208, 109350. doi:10.1016/j.petrol.2021.109350

Hou, H., Shao, L., Liang, G., Tang, Y., Zhang, H., and Zhang, J. (2022b). Repeated wildfires in the middle jurassic Xishanyao formation (aalenian and bajocian ages) in northwestern China. *Acta Geol. Sin.* 96, 1752–1763. doi:10.1111/1755-6724.14912

Hu, G., Zhang, S., Li, J., Li, J., and Han, Z. (2010). The origin of natural gas in the Hutubi gas field, Southern Junggar Foreland Sub-basin, NW China. *Int. J. Coal Geol.* 84, 301–310. doi:10.1016/j.coal.2010.10.009

Jasinge, D., Ranjith, P. G., and Choi, S. K. (2011). Effects of effective stress changes on permeability of latrobe valley Brown coal. *Fuel* 90, 1292–1300. doi:10.1016/j.fuel.2010.10.053

Jiang, B., Qu, Z., Wang, G. G. X., and Li, M. (2010). Effects of structural deformation on formation of coalbed methane reservoirs in Huaibei coalfield, China. *Int. J. Coal Geol.* 82, 175–183. doi:10.1016/j.coal.2009.12.011

Kang, J., Fu, X., Elsworth, D., and Liang, S. (2020). Vertical heterogeneity of permeability and gas content of ultra-high-thickness coalbed methane reservoirs in the southern margin of the Junggar Basin and its influence on gas production. *J. Nat. Gas Sci. Eng.* 81, 103455. doi:10.1016/j.jngse.2020.103455

Kang, J., Fu, X., Gao, L., and Liang, S. (2018). Production profile characteristics of large dip angle coal reservoir and its impact on coalbed methane production: A case study on the Fukang west block, southern Junggar Basin, China. *J. Petroleum Sci. Eng.* 171, 99–114. doi:10.1016/j.petrol.2018.07.044

Kang, J., Fu, X., Shen, J., Liang, S., Chen, H., and Shang, F. (2022). Characterization of coal structure of high-thickness coal reservoir using geophysical logging: A case study in southern Junggar Basin, Xinjiang, northwest China. *Natural Resources Research.* 31, 929–951, doi:10.1007/s11053-022-10018-x

Karacan, C. Ö., and Okandan, E. (2000). Fracture/cleat analysis of coals from Zonguldak Basin (northwestern Turkey) relative to the potential of coalbed methane production. *Int. J. Coal Geol.* 44, 109–125. doi:10.1016/s0166-5162(00)00004-5

Karacan, C. Ö., Ruiz, F. A., Cotè, M., and Phipps, S. (2011). Coal mine methane: A review of capture and utilization practices with benefits to mining safety and to greenhouse gas reduction. *Int. J. Coal Geol.* 86, 121–156. doi:10.1016/j.coal.2011.02.009

Li, G., Yan, D., Zhuang, X., Zhang, Z., and Fu, H. (2019). Implications of the pore pressure and *in situ* stress for the coalbed methane exploration in the southern Junggar Basin, China. *Eng. Geol.* 262, 105305. doi:10.1016/j.enggeo.2019.105305

Li, H., and Ogawa, Y. (2001). Pore structure of sheared coals and related coalbed methane. *Environ. Geol.* 40, 1455–1461. doi:10.1007/s002540100339

Li, H., Ogawa, Y., and Shimada, S. (2003). Mechanism of methane flow through sheared coals and its role on methane recovery☆. *Fuel* 82, 1271–1279. doi:10.1016/s0016-2361(03)00020-6

Li, J., Pan, D., Cui, R., Ding, E., Zhang, W., and Hu, M. (2016). Prediction of tectonically deformed coal based on lithologic seismic information. *J. Geophys. Eng.* 13, 116–122. doi:10.1088/1742-2132/13/1/116

Li, L., Liu, D., Cai, Y., Wang, Y., and Jia, Q. (2021). Coal structure and its implications for coalbed methane exploitation: A review. *Energy fuels.* 35, 86–110. doi:10.1021/acs.energyfuels.0c03309

Li, W., Li, X., Zhao, S., Li, J., Lu, S., Liu, Y., et al. (2022). Evaluation on carbon isotope fractionation and gas-in-place content based on pressure-holding coring technique. *Fuel* 315, 123243. doi:10.1016/j.fuel.2022.123243

Li, X., Fu, X., Yang, X., Ge, Y., and Quan, F. (2018). Coalbed methane accumulation and dissipation patterns: A case study of the Junggar Basin, NW China. *J. Asian Earth Sci.* 160, 13–26. doi:10.1016/j.jseaes.2018.04.003

Li, Y., Zhang, C., Tang, D., Gan, Q., Niu, X., Wang, K., et al. (2017). Coal pore size distributions controlled by the coalification process: An experimental study of coals from the Junggar, Ordos and Qinshui basins in China. *Fuel* 206, 352–363. doi:10.1016/j.fuel.2017.06.028

Liu, A., Fu, X., Wang, K., An, H., and Wang, G. (2013). Investigation of coalbed methane potential in low-rank coal reservoirs - free and soluble gas contents. *Fuel* 112, 14–22. doi:10.1016/j.fuel.2013.05.032

Liu, S., and Harpalani, S. (2013). Permeability prediction of coalbed methane reservoirs during primary depletion. *Int. J. Coal Geol.* 113, 1–10. doi:10.1016/j.coal.2013.03.010

Meng, Z., Zhang, J., and Wang, R. (2011). *In-situ* stress, pore pressure and stress-dependent permeability in the Southern Qinshui Basin. *Int. J. Rock Mech. Min. Sci. (1997).* 48, 122–131. doi:10.1016/j.ijrmms.2010.10.003

Moore, T. A. (2012). Coalbed methane: A review. *Int. J. Coal Geol.* 101, 36–81. doi:10.1016/j.coal.2012.05.011

Niu, Q., Cao, L., Sang, S., Wang, W., Zhou, X., Yuan, W., et al. (2021). Experimental study on the softening effect and mechanism of anthracite with CO2 injection. *Int. J. Rock Mech. Min. Sci. (1997).* 138, 104614. doi:10.1016/j.ijrmms.2021.104614

Niu, Q., Wang, Q., Wang, W., Chang, J., Chen, M., Wang, H., et al. (2022). Responses of multi-scale microstructures, physical-mechanical and hydraulic characteristics of roof rocks caused by the supercritical CO2-water-rock reaction. *Energy* 238, 121727. doi:10.1016/j.energy.2021.121727

Ou, C., Li, C., Zhi, D., Xue, L., and Yang, S. (2018). Coupling accumulation model with gas-bearing features to evaluate low-rank coalbed methane resource potential in the southern Junggar Basin, China. *Am. Assoc. Pet. Geol. Bull.* 102, 153–174. doi:10.1306/03231715171

Palmer, I., and John, M. (1998). How permeability depends on stress and pore pressure in coalbeds: A new model. *SPE Reserv. Eval. Eng.* 1, 539–544. doi:10.2118/52607-pa

Palmer, I. (2009). Permeability changes in coal: Analytical modeling. *Int. J. Coal Geol.* 77, 119–126. doi:10.1016/j.coal.2008.09.006

Pan, J., Lv, M., Hou, Q., Han, Y., and Wang, K. (2019). Coal microcrystalline structural changes related to methane adsorption/desorption. *Fuel* 239, 13–23. doi:10.1016/j.fuel.2018.10.155

Pan, J., Zhu, H., Hou, Q., Wang, H., and Wang, S. (2015). Macromolecular and pore structures of Chinese tectonically deformed coal studied by atomic force microscopy. *Fuel* 139, 94–101. doi:10.1016/j.fuel.2014.08.039

Pan, Z., Connell, L. D., and Camilleri, M. (2010). Laboratory characterisation of coal reservoir permeability for primary and enhanced coalbed methane recovery. *Int. J. Coal Geol.* 82, 252–261. doi:10.1016/j.coal.2009.10.019

Pan, Z., and Connell, L. D. (2011). Modelling of anisotropic coal swelling and its impact on permeability behaviour for primary and enhanced coalbed methane recovery. *Int. J. Coal Geol.* 85, 257–267. doi:10.1016/j.coal.2010.12.003

Pashin, J. C. (2010). Variable gas saturation in coalbed methane reservoirs of the Black Warrior Basin: Implications for exploration and production. *Int. J. Coal Geol.* 82, 135–146. doi:10.1016/j.coal.2009.10.017

Pillalamarry, M., Harpalani, S., and Liu, S. (2011). Gas diffusion behavior of coal and its impact on production from coalbed methane reservoirs. *Int. J. Coal Geol.* 86, 342–348. doi:10.1016/j.coal.2011.03.007

Rice, C. A., Flores, R. M., Stricker, G. D., and Ellis, M. S. (2008). Chemical and stable isotopic evidence for water/rock interaction and biogenic origin of coalbed methane, Fort Union Formation, Powder River Basin, Wyoming and Montana U.S.A. *Int. J. Coal Geol.* 76, 76–85. doi:10.1016/j.coal.2008.05.002

Rice, D. D. (1993). Composition and origins of coalbed gas, 159–184. *SG 38: Hydrocarbons from coal.* U.S. Department of Energy Office of Scientific and Technical Information USA

Scott, S., Anderson, B., Crosdale, P. J., Dingwall, J., and Leblang, G. (2007). Coal petrology and coal seam gas contents of the Walloon Subgroup -Surat Basin, Queensland, Australia. *Int. J. Coal Geol.* 70, 209–222. doi:10.1016/j.coal.2006.04.010

Smyth, M., and Buckley, M. J. (1993). Statistical analysis of the microlithotype sequences in the Bulli Seam, Australia, and relevance to permeability for coal gas. *Int. J. Coal Geol.* 22, 167–187. doi:10.1016/0166-5162(93)90025-6

Wang, B., Li, J., Zhang, Y., Wang, H., Liu, H., Li, G., et al. (2009). Geological characteristics of low rank coalbed methane, China. *Petroleum Explor. Dev.* 36, 30–34. doi:10.1016/s1876-3804(09)60108-7

Wang, Q., Xu, H., Tang, D., Yang, S., Wang, G., Ren, P., et al. (2022). Indication of origin and distribution of coalbed gas from stable isotopes of gas and coproduced water in Fukang area of Junggar Basin, China. *Am. Assoc. Pet. Geol. Bull.* 106, 387–407. doi:10.1306/09152120028

Wang, Z., Pan, J., Hou, Q., Niu, Q., Tian, J., Wang, H., et al. (2018). Changes in the anisotropic permeability of low-rank coal under varying effective stress in Fukang mining area, China. *Fuel* 234, 1481–1497. doi:10.1016/j.fuel.2018.08.013

Whiticar, M. J. (1999). Carbon and hydrogen isotope systematics of bacterial formation and oxidation of methane. *Chem. Geol.* 161, 291–314. doi:10.1016/s0009-2541(99)00092-3

Whiticar, M. J. (1996). Stable isotope geochemistry of coals, humic kerogens and related natural gases. *Int. J. Coal Geol.* 32, 191–215. doi:10.1016/s0166-5162(96)00042-0

Wu, Q. (1989). Structural evolution and prospects of Junggar Basin. *Xinjiang Geol.* 4, 1–19.

Xu, C., Yang, G., Wang, K., and Fu, Q. (2021). Uneven stress and permeability variation of mining-disturbed coal seam for targeted CBM drainage: A case study in Baode coal mine eastern Ordos Basin China, 289. 119911: .*Fuel* doi:10.1016/j.fuel.2020.119911

Yang, Q., Liu, D. M., Huang, W. H., Che, Y., Hu, B. L., and Wei, Y. J. (2005). *Coalbed methane geology and resources comprehensive evaluation in northwest China*. Beijing, China: Geological Publication House.

Yang, S., and Tian, J. (2011). Characteristics of CBM reservoir in eastern part of Junggar Basin. *China Coalbed Methane* 8, 21–23.

Yao, Y., Liu, D., and Qiu, Y. (2013). Variable gas content, saturation, and accumulation characteristics of Weibei coalbed methane pilot-production field

in the southeastern Ordos Basin, China. *Am. Assoc. Pet. Geol. Bull.* 97, 1371–1393. doi:10.1306/02131312123

Yin, H. (2009). Prospect of exploration of CBM resources in Fukang coal mining area in Xinjiang and recommendations on its development. *China Coalbed Methane* 6, 16–18.

Yu, Y., and Wang, Y. (2020). Characteristics of low-rank coal reservoir and exploration potential in Junggar Basin: New frontier of low-rank CBM exploration in China. *J. Pet. Explor. Prod. Technol.* 10, 2207–2223. doi:10.1007/s13202-020-00923-3

Zhang, B., Deng, Z., Fu, X., and Yin, K. (2021). A study on three-phase gas content in coal reservoirs and coalbed methane-water differential distribution in the western Fukang mining area, Xinjiang, China. *ACS Omega* 6, 3999–4012. doi:10.1021/acsomega.0c05930

Zhang, T., Tao, S., Tang, D., Tang, S., Xu, H., Zhang, A., et al. (2021). Permeability anisotropy in high dip angle coal seam: A case study of southern Junggar Basin. *Nat. Resour. Res.* 30, 2273–2286. doi:10.1007/s11053-021-09831-7

Zhao, J., Tang, D., Xu, H., Li, Y., Li, S., Tao, S., et al. (2016). Characteristic of *in situ* stress and its control on the coalbed methane reservoir permeability in the eastern margin of the Ordos Basin, China. *Rock Mech. Rock Eng.* 49, 3307–3322. doi:10.1007/s00603-016-0969-1

Zhi, D., Xue, l., Wang, Y., Ou, C., Peng, W., Yang, D., et al. (2013). *Coalbed methane resource and exploration potential in Junggar Basin*. Beijing, China: Petroleum Industry Press.

Zhou, S., Liu, D., Cai, Y., and Yao, Y. (2016). Gas sorption and flow capabilities of lignite, subbituminous and high-volatile bituminous coals in the Southern Junggar Basin, NW China. *J. Nat. Gas Sci. Eng.* 34, 6–21. doi:10.1016/j.jngse.2016.06.039